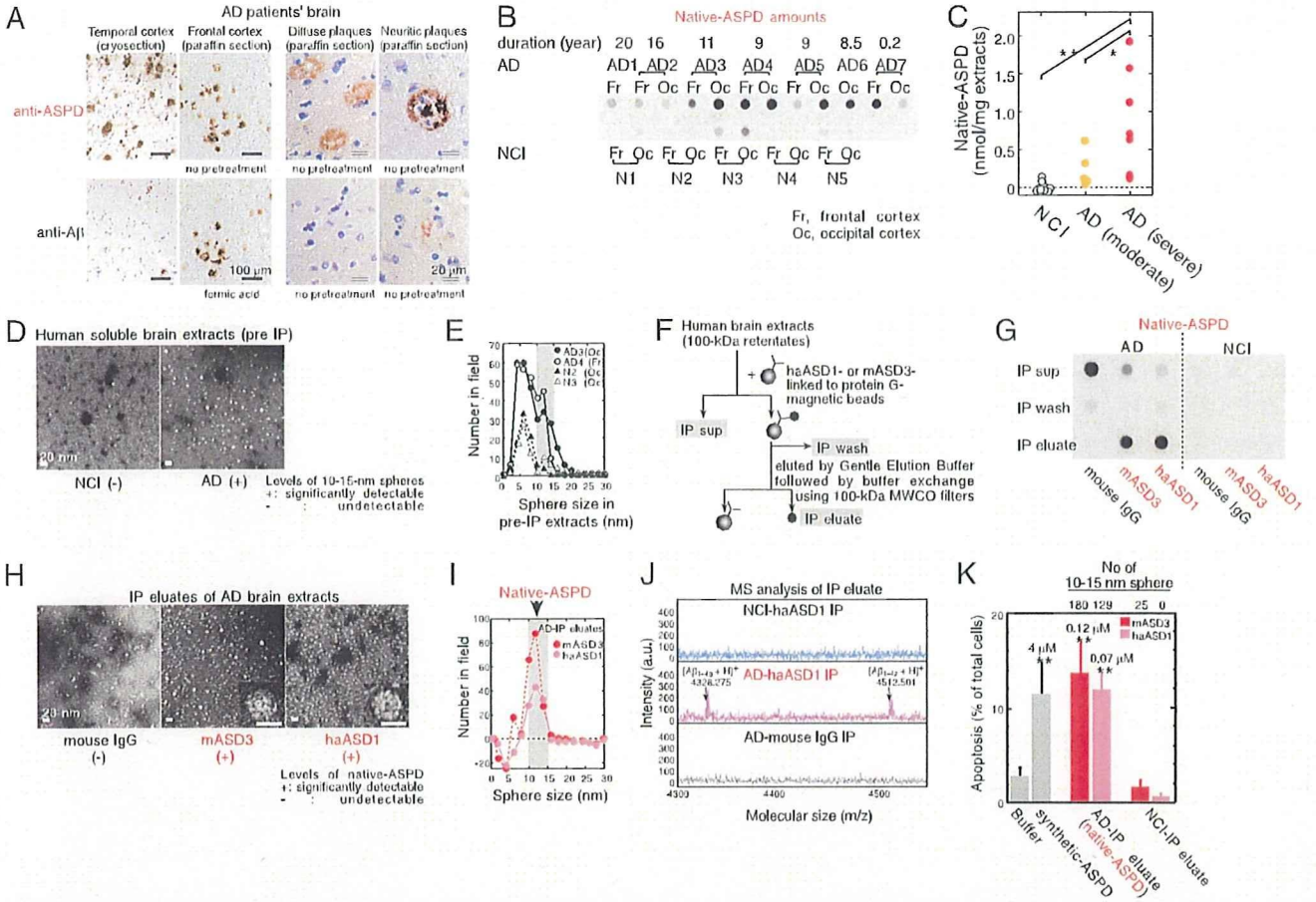

FIGURE 2. **Isolation of native ASPDs.** *A*, AD brains were stained with rpASD1 (5 μg/ml) or anti-Aβ1–42 C-terminal antibody (0.5 μg/ml; 2 μg/ml for cryosections). *B* and *C*, dot blotting of 100-kDa retentates (>100 kDa) of AD or NCI brain extracts (1 μg of soluble extracts/dot) using rpASD1 (Scheffé post hoc test; **, $p = 0.0011$; *, $p = 0.0388$). *Fr*, frontal cortex; *Oc*, occipital cortex. *D* and *E*, TEM images (*D*) and particle analysis of 100-kDa retentates ($n = 3$; 10 randomly selected fields) (*E*). *F* and *G*, method for immunoprecipitation (*IP*) (*F*) and dot blotting (using rpASD1) of IP supernatants (*sup*), wash, and eluate fractions. IPs were performed using haASD1, mASD3, or mouse IgG (*G*). *H* and *I*, TEM images (*inset*, *bar*, 10 nm) (*H*) and particle analysis of IP eluates ($n = 3$; 15 randomly selected fields, background (a small amount of spheres <10 nm contained in eluate with buffers)-subtracted data are shown) (*I*). *J*, representative MALDI-TOF/MS data. Aβ-(1–40) and Aβ-(1–42) were detected only in native ASPDs at theoretical monoisotopic mass values ($([Aβ\text{-}(1–40) + H]^+$, 4328 Da; $[Aβ\text{-}(1–42) + H]^+$, 4512 Da) as observed in synthetic Aβ peptides. *K*, toxicity of isolated native ASPDs toward primary rat septal neurons (mean ± S.D.; Scheffé post hoc test, **, $p < 0.0001$, compared with buffer, $n > 8$) correlated with the 10–15-nm sphere number determined as in *I*. Neurons treated with NCI-IP eluates showed only background levels of apoptosis similar to those of neurons treated with buffers. *Inset*, synthetic or native ASPD amounts in Aβ monomer concentrations.

with insoluble fractions of AD brains extracted with SDS or formic acid (supplemental Fig. S3*A*). Furthermore, this insoluble fraction produced broad smears in Western blots of Aβ, as is usually observed with fibrils (42) (supplemental Fig. S3*B*). In contrast, the ASD antibodies reacted only with soluble fractions of AD brains (supplemental Fig. S3*A*) in which the human ASPD counterpart was actually present, as described below (see under "Isolation of Native ASPD from Brains of AD Patients"). These results collectively indicate that the ASD antibodies detect a human ASPD counterpart, namely native ASPD, associated with plaques and neurites in AD brains. In subsequent work, we used monoclonal mASD3 and haASD1 for isolating ASPDs, because of their high affinity, and polyclonal rpASD1 for detecting ASPDs (except Fig. 3*A*; see also "Immunoprecipitations" under "Experimental Procedures").

Isolation of Native ASPD from Brains of AD Patients—The tissue fractionation study revealed that native ASPDs are recovered in soluble fractions of AD brains. To investigate the amount of native ASPD, we prepared soluble fractions of AD brains ($n = 7$; age 85.6 ± 3.1 years, brain weight 1025 ± 104 g) and NCI ($n = 5$; age 72.6 ± 9.5 years, brain weight 1236 ± 64 g) by means of a nondenaturing procedure using solutions of physiologic ionic strength and pH without detergents. We then obtained 100-kDa retentates of the soluble fractions to concentrate native ASPDs (larger than 100 kDa) and to eliminate other Aβ assemblies smaller than 100 kDa (as performed in Fig. 1*A*). The 100-kDa retentates of AD brains thus obtained had high levels of rpASD1-reactive substances, but those of NCI brains had very low or negligible reactivity (Fig. 2*B*). Consistent with the above data, much higher numbers of spheres sized 10–15 nm were present in 100-kDa retentates of AD patients than in those of NCI (Fig. 2, *D* and *E*). These results suggest that rpASD1-reactive 10–15-nm spheres in 100-kDa retentates of AD are native ASPD candidates. We then immunoisolated native ASPDs (Fig. 2*F*) from large amounts of AD-derived 100-kDa retentates using two monoclonal antibodies, haASD1 and mASD3 (Fig. 2, *G–J*). These antibodies were chosen for their extremely high affinity for ASPD ($K_d < 10^{-12}$ M) and for their

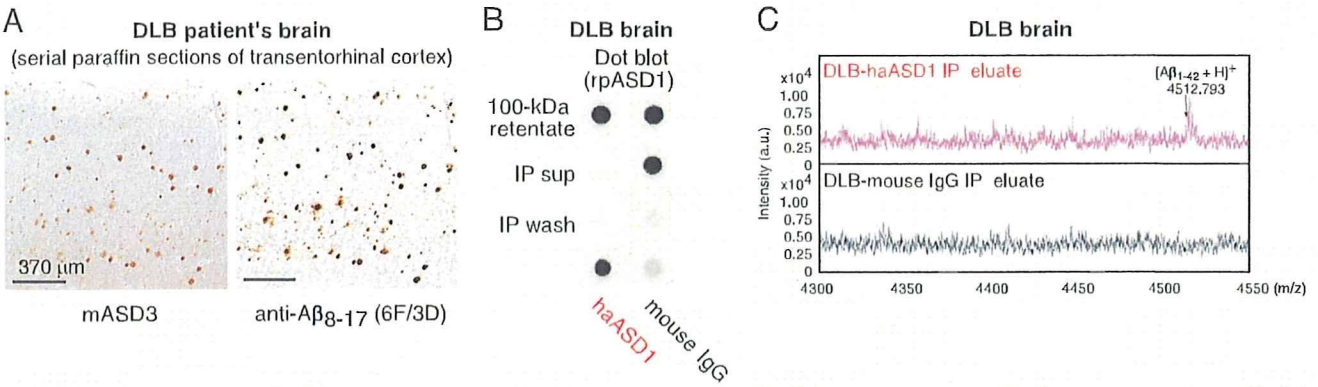

FIGURE 3. **Native ASPDs exist in DLB brains.** *A*, immunostaining using mASD3 (2.5 μg/ml) and anti-Aβ8–17 (pretreated with formic acid; 1:100; DAKO). *B*, IP was performed with haASD1 or mouse IgG as in Fig. 2*F* using 100-kDa retentates (4 μg of soluble brain extracts/IP). Dot blotting (0.04 μg/ml rpASD1) of 100-kDa retentates (2 μg of soluble brain extracts/dot), IP supernatants (*sup*), wash, and eluate is shown. *C*, representative MALDI-TOF/MS data.

recognition of different epitopes (Table 1). Judging from the results of quantification of dot blots using rpASD1 (Fig. 2*G*), we obtained about 43 pmol of native ASPDs (expressed as Aβ monomer concentration) from 1 g of AD brain tissues ($n = 6$). The rpASD1 reactivity in the IP eluates was considered to be mostly due to the 10–15-nm spheres, because the number of spheres counted by TEM (Fig. 2*H*) (1.0×10^{10} 10–15-nm sphere/μl estimated from the number of spheres in Fig. 2*K*, $n = 6$) was very similar to the amount of rpASD1-reactive ASPD obtained from dot blots (1.1×10^{10} native ASPD/μl based on the ASPD concentration in Fig. 2*K*, $n = 8$). This means that rpASD1-reactive 10–15-nm spheres were selectively isolated by a combination of 100-kDa retention and IP. Indeed, as shown by the TEM data (Fig. 2*H*), the non-ASPD small-sized spheres (<10 nm) that had been present in large amounts in 100-kDa retentates of AD and NCI were largely eliminated by the IP procedure (compare Fig. 2, *I* with *E*). Accordingly, we successfully isolated native ASPDs, consisting of 10–15-nm spheres (>95%; Fig. 2, *H* and *I*), from 100-kDa retentates of AD. In contrast, native ASPD-like assemblies were scarcely detected in IP eluates from 100-kDa retentates of NCI (Fig. 2, *G* and *K*). We next examined whether native ASPDs consisted of Aβ. Mass spectrometric analysis showed that singly charged ions corresponding to Aβ-(1–42) and Aβ-(1–40) were detected in native ASPDs (Fig. 2*J*). These results collectively demonstrate that 10–15-nm spherical Aβ assemblies isolated from AD brains are native ASPDs. Notably, anti-pan Aβ 6E10 could not immunoisolate native ASPDs (data not shown), probably because of its weak affinity for ASPDs ($K_d \approx 10^{-9}$ M) compared with ASD antibodies ($K_d < 10^{-12}$ M) (Table 1). We also confirmed that anti-pan oligomer A11 antibody failed to detect native ASPDs (supplemental Fig. S4).

Having isolated native ASPDs selectively from human AD brains, we next examined whether they elicited neurodegeneration of rat primary neuronal cells. Surprisingly, AD-derived native ASPDs were even more toxic than synthetic ASPDs (Fig. 2*K*). These results collectively demonstrate that we have newly isolated A11-negative, high mass assemblies that cause neuronal cell death and that differ in mass and surface tertiary structure from other reported nonfibrillar Aβ assemblies.

Native ASPD Amount Correlates with the Pathologic Severity of AD—We next examined whether the amount of native ASPD correlated with the pathologic severity of AD brains. Larger amounts of native ASPD were present in AD patients with severe pathology (diagnosed "C" according to the CERAD criteria (43)) than in AD patients with moderate pathology (diagnosed "B") (Fig. 2*C*). Furthermore, in AD patients with severe pathology, significantly higher amounts of native ASPD were detected in the frontal or temporal cortices (7.2 ± 1.5 nmol/g brain tissue, $n = 3$, Scheffé post hoc test $p = 0.0012$) than in the cerebellum (0.14 ± 0.1 nmol/g brain tissue). The result is consistent with previous findings that the cerebellum in AD is pathologically less affected (44, 45).

The above observations suggest the involvement of native ASPDs in neurodegeneration of AD brains. We therefore examined brains of patients suffering from DLB, the second most frequent cause of cognitive decline associated with neurodegeneration in the elderly (46, 47), because the majority of DLB brains have been shown to have AD-type pathology, including plaques (46–48). Interestingly, native ASPDs were also isolated from DLB brains (Fig. 3, *A–C*).

AD-derived Native ASPDs Cause Severe Degeneration of Human Neuronal Cells—To further elucidate the relationship between neuronal loss and native ASPDs, we first examined whether native ASPDs induce degeneration of human mature neuronal cells. Because studies using human primary neurons are problematic for ethical and practical reasons, cells with neuronal properties were induced from human bone marrow stromal cells (MSCs) (49). Initially, postmitotic neuronal cells were induced from human MSCs (>95% were neuron-specific MAP2ab-positive cells without glia) (49). Treatment of these cells with glial cell line-derived neurotrophic factor promoted their maturation into functional neuronal cells (49). We found that a 2-day treatment of the human MSC-derived functional neuronal cells with isolated native ASPDs caused severe degeneration, whereas IP eluates from NCI brains had no effect (Fig. 4*A*). In addition, pretreatment with mASD3 antibody (100 μg/ml) significantly blocked this toxicity (Fig. 4*A*), as observed in the case of the 158–669-kDa ASPDs (supplemental Fig. S5*A*), dem-

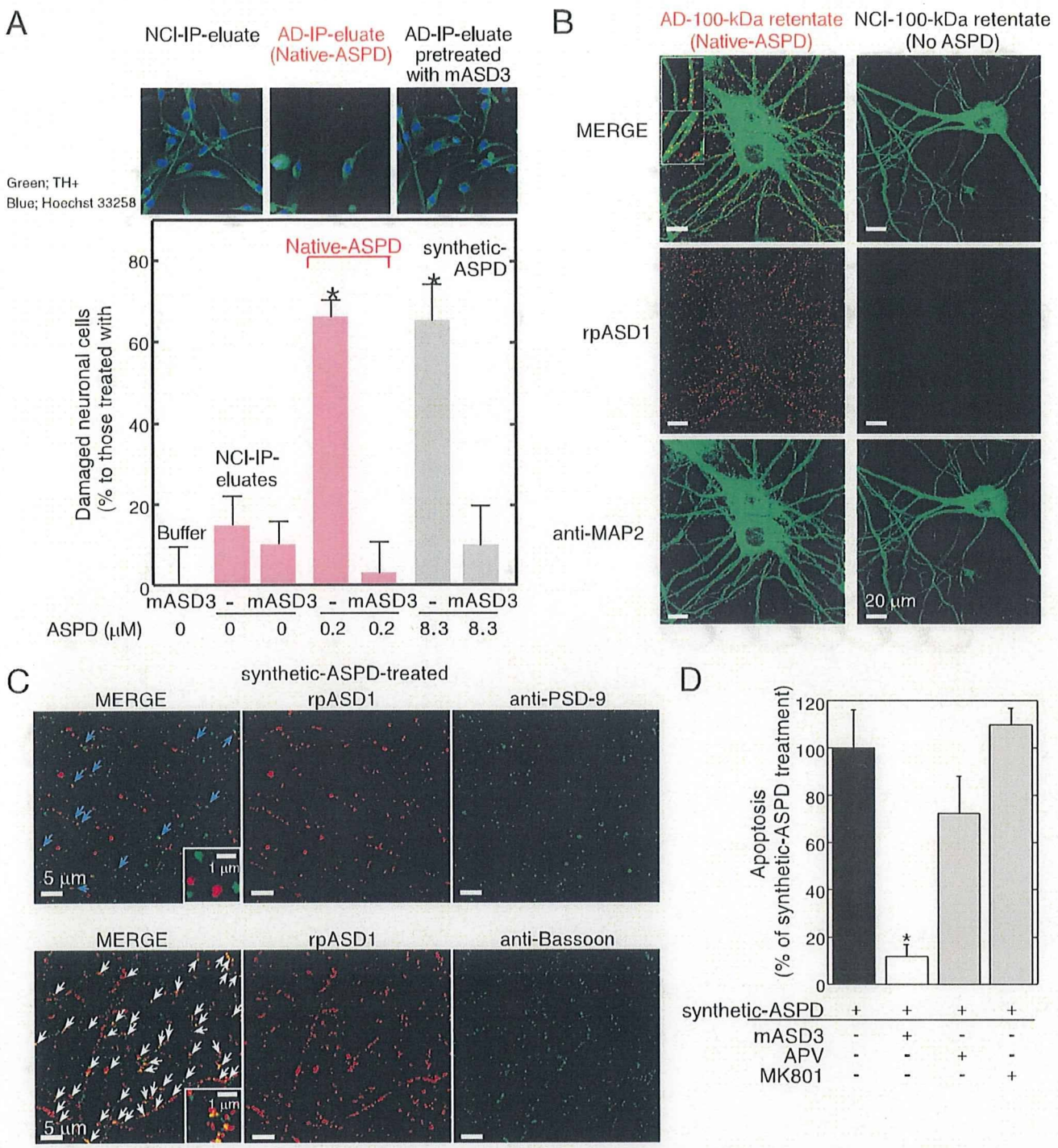

FIGURE 4. **Characterization of native and synthetic ASPD-induced toxicity.** *A*, IP was performed using haASD1 as in Fig. 2*F*. Human neuronal cells were treated for 2 days with AD or NCI-IP eluates, with or without 2-h mASD3 (100 μg/ml) pretreatment. Nondamaged cells were counted after tyrosine hydroxylase (*TH*+) and Hoechst 33258 staining. The ratio of damaged cells to neuronal cells treated with buffer alone (mean ± S.D.) is shown (Scheffé post hoc test; *, $p < 0.0001$, $n = 5$). Neuronal cells treated with mASD3 alone or NCI-IP eluates showed only background levels of damaged cells similar to those in the case of cells treated with buffer. *B* and *C*, mature rat hippocampal neurons (24 DIV in *B* and 19 DIV in *C*) were incubated for 30 min either with 100-kDa retentates of AD (containing 0.8 μM native ASPDs) or NCI (no native ASPD detected) brain extracts in *B* or with 0.5 μM 158–669-kDa ASPDs (prepared from Aβ-(1–42); see Fig. 1*A*) in *C*. Bound ASPDs were detected by rpASD1, as in Fig. 1*D*. Punctate labeling was found primarily on neurites and surrounding cell bodies of neurons treated with native or synthetic ASPDs, but it was hardly detectable in neurons treated with the NCI retentates. A representative high power view is shown in the *inset* (*B*; *bar*, 5 μm). Neurons were co-stained with an antibody against anti-MAP2 in *B*, against a postsynaptic marker PSD-95 in *C* (*upper panels*), or against a presynaptic marker bassoon in *C* (*lower panels*). Z-stack images are shown (except *lower panels* in *C*) as in Fig. 1*D*. Bound ASPDs did not co-localize with PSD-95 but were concentrated with bassoon (*white arrows* in *C*), although they were occasionally localized in close proximity to PSD-95 (*blue arrows* in *C*). *D*, mature rat hippocampal neurons (21 DIV) were treated with 1 μM 158–669-kDa ASPDs for 2 days, with or without pretreatment (100 μg/ml mASD3 for 2 h; competitive (APV) or uncompetitive (MK801) NMDA-R antagonists (10 μM) for 30 min). Data represent mean ± S.D. (Scheffé post hoc test; *, $p = 0.0039$, compared with synthetic ASPDs; synthetic ASPDs, $n = 7$; synthetic ASPDs + APV or MK801, $n = 5$; synthetic ASPDs + mASD3, $n = 4$).

onstrating that the observed neuronal cell death was caused by native ASPDs.

We then examined whether native ASPDs bind mature rat hippocampal neurons, as is observed in the case of synthetic ASPDs (Fig. 1*D* and supplemental Fig. S5*B*). Binding of AD-derived native ASPDs to 24-DIV mature rat hippocampal neurons was detected with rpASD1 most intensely in neurites and also to some extent in cell bodies (Fig. 4*B*). These results suggest that, despite the difference in dose dependence of neurotoxicity (Figs. 2*K* and 4*A*), native and synthetic ASPDs share essentially the same mechanism of neurotoxicity, *i.e.* they have the same surface tertiary structure that is responsible for exerting the toxicity. We speculate that the apparent difference in dose dependence might be attributed to differences in molecular compositions, but testing this idea will require further analyses using large amounts of isolated native ASPDs.

Mode of Native ASPD Neurotoxicity Is Different from That of Other Reported Aβ Assemblies—The above results (Fig. 4, *A* and *B*) show that native ASPDs cause neuronal cell death, possibly by binding to neuronal cell surfaces. We therefore examined ASPD-binding sites on mature neurons to elucidate the molecular basis of native ASPD neurotoxicity. As shown in the high power images in Fig. 4*B* (*inset*), bound native ASPDs appeared to protrude from the MAP2 staining of dendrites. Essentially the same results were obtained with the binding of synthetic ASPDs (supplemental Fig. S5*B* (*inset*)). Because of the limited availability of native ASPDs, we employed synthetic ASPDs for further analysis, as synthetic and native ASPDs share essential properties. Consistent with the above observation, the binding of synthetic ASPDs did not co-localize with a postsynaptic marker, PSD-95 (Fig. 4*C*, *upper panel*), although it was occasionally detected in close proximity to PSD-95 (*blue arrows* in *C*). Instead, ASPD-binding sites appeared to be concentrated at presynaptic sites stained by the antibody against a presynaptic marker, bassoon (*white arrows* in Fig. 4*C*, *lower panel*).

Although previous studies using cell or slice culture systems have found that Aβ assemblies such as dimers, ADDLs and AβOs bind postsynapses and depend on postsynaptic signaling mechanisms for exerting synaptotoxicity (23), the presynaptic binding of ASPDs apparent in Fig. 4*B* suggests that ASPD neurotoxicity would not require postsynaptic signaling mechanisms such as the *N*-methyl-D-aspartate glutamate receptor (NMDA-R) pathway. Indeed, neither a competitive (APV) nor an uncompetitive (MK801) NMDA-R antagonist inhibited synthetic ASPD-induced neurodegeneration (Fig. 4*D*). As noted above, native and synthetic ASPDs share the common surface tertiary structure responsible for exerting the toxicity. Therefore, the findings obtained with synthetic ASPDs (Fig. 4, *C* and *D*) strongly suggest that native ASPDs cause neuronal cell death through presynaptic target(s) on mature neurons. Furthermore, these observations are consistent with the findings indicating that native ASPDs have a distinct surface tertiary structure from other reported Aβ assemblies and support the hypothesis that native ASPDs have a different target(s) from other Aβ assemblies.

DISCUSSION

Aβ assemblies are considered to acquire surface tertiary structures that are not present in physiologic Aβ monomers and that induce synaptic impairment and neuronal loss through interactions with neuronal cells. Therefore, as recently suggested (12), it is reasonable to classify seemingly different Aβ assemblies in terms of their immunoreactivity to antibodies that recognize particular surface tertiary structure. Because the surface tertiary structure mediates the binding of Aβ assemblies to their target(s) and is therefore responsible for exerting the toxic effects, Aβ assemblies having distinct surface tertiary structures are likely to have distinct mechanisms of neurotoxicity and may contribute differently to the disease development. Here we have demonstrated the existence of patient-derived native ASPDs by selectively immunoisolating them from AD and DLB brains (Figs. 2 and 3) using ASPD tertiary structure-dependent antibodies (Fig. 1 and Table 1). The native ASPDs (>100 kDa) thus obtained are larger in mass than AD-derived Aβ dimers and other reported assemblies such as 12-mers (53~60 kDa; ADDLs, globulomer, Aβ*56) or AβOs (~90 kDa) (supplemental Table S1). More importantly, native ASPDs are considered to have a distinct surface tertiary structure from those other assemblies because they differ in immunospecificity, as illustrated by the fact that ASPD tertiary structure-dependent antibodies showed minimal reactivity with the 100-kDa filtrate containing monomers and dimers (Fig. 1*A*) or with ADDLs (supplemental Fig. S1*A*) (16) in dot blots. Additionally, anti-pan oligomer A11 antibody (22) recognized AβOs but not synthetic ASPDs (Fig. 1*B*) or native ASPDs (supplemental Fig. S4). Finally, anti-Aβ N-terminal antibodies such as 82E1 blocked the synaptotoxicity of AD-derived dimers (30) but failed to block synthetic ASPD-induced neurodegeneration (supplemental Fig. S5*A*). These results all indicate a difference in the surface tertiary structure between these assemblies and ASPDs.

As for the cellular basis of the Aβ-induced synaptic changes, previous studies have suggested the involvement of postsynaptic signaling mechanisms (23). For example, the binding of ADDLs and AβOs has been reported to co-localize with PSD-95 (19, 23). As expected from the postsynaptic locale of their binding, ADDLs bind close to or at NMDA-R (23), and NMDA-R antagonists inhibit ADDL-induced dendritic changes (23), reactive oxygen species formation (50), and insulin receptor impairment (51). NMDA-R antagonists have also been reported to inhibit Aβ dimer-induced synaptic loss (24, 30). Interestingly, cellular prion protein, which interacts with NMDA-R (52), has recently been reported to serve as a high affinity postsynaptic receptor mediating ADDL-induced synaptic dysfunction (53). Taken together, these studies are consistent with the idea that Aβ dimers, ADDLs, and AβOs perturb postsynaptic transmission (19, 23, 30).

We found that, unlike the above Aβ assemblies, ASPDs bind presynaptic target(s) on neurons to induce neurodegeneration (Fig. 4, *A–C*). This may be reasonable in view of the distinct ASPD surface tertiary structure. Although the actual targets of native ASPDs remain to be elucidated, native ASPDs seem to affect mature neuron-specific molecules or cellular pathways,

as synthetic ASPD-induced neurotoxicity appeared to be confined to neurons, being especially active toward mature neurons, but sparing non-neuronal cells and immature neurons (supplemental Fig. S6, *A–C*). Together, the findings indicate that native ASPDs are patient-derived, A11-negative, high mass Aβ assemblies with a distinct toxic surface that binds presynaptic target(s) on mature neurons, leading to neuronal loss (supplemental Table S1). Although further studies are required to reveal how native ASPDs exert neurotoxicity in the brains of patients with AD, our findings indicate for the first time that presynaptic signaling mechanisms may play a critical role in Aβ-induced neurodegeneration in AD.

Recent *in vivo* as well as *in vitro* studies support the toxicity of nonfibrillar Aβ assemblies and their possible causative roles in the neuropathology of AD (54–56), which is consistent with the dissociation between fibril load and cognitive decline in patients with AD (32, 57, 58). Thus, Aβ assemblies other than fibrils have been considered to be the preferred therapeutic targets for AD (54). However, the nature of the Aβ species and the oligomer state responsible for the pathogenesis remain controversial because of the heterogeneity of Aβ assemblies in terms of Aβ species and oligomer size. It is also unknown how Aβ monomers assemble into oligomers in living human brains. Nevertheless, previous *in vitro* studies have shown that Aβ monomers develop into a variety of assemblies that might represent distinct structural variants (10–13). These studies suggest that assembly may not be a linear process but may be the result of a series of multiple processes involving intermediates from side paths. Taking all the results together, it seems reasonable to assume that the brains of patients with AD contain distinct types of Aβ assemblies with different surface tertiary structures that may play different roles in AD development. Therefore, identification and characterization of all types of Aβ assemblies actually present in brains from humans with AD will be important for understanding the molecular mechanisms underlying the AD progression from the initial step to the symptomatic phase and for the development of therapies based on this understanding. Fractionation studies using oligomer tertiary structure-dependent antibodies as shown here will help to elucidate the assembly process and to determine the Aβ assembly state causing the pathogenesis. We have isolated native ASPDs that cause degeneration of mature human neuronal cells *in vitro* (Fig. 4*A*) and have shown that the amount of native ASPD is correlated with the pathologic severity of clinically proven AD cases (Fig. 2*C*).

These findings suggest that native ASPDs might be a candidate for Aβ assemblies that directly cause neuronal loss in the brains of humans with AD. However, it remains to be elucidated whether or not ASPDs play a particular role in the onset or early stage of disease development. Braak and coworkers (59) have compared the expansion of Aβ pathology in whole brain regions between AD cases and nondemented cases with or without Aβ-related pathology. They found that patients with clinically proven AD exhibit late Aβ stages, although the nondemented cases with AD-related pathology show early Aβ stages. Their findings suggest that AD brains develop pathologic Aβ deposition before clinical symptoms become apparent, and this may start much earlier in nondemented patients with AD-related Aβ pathology. Quantitative studies, with the assistance of clinicians, on the brains of people in different Aβ stages, including nondemented people with AD-related Aβ pathology, will be helpful to elucidate if ASPDs play a role in neuronal loss in AD from the early stage of disease development.

Analyses on brains of APP-transgenic mice with or without neuronal loss would also help to elucidate the relationship between ASPDs and neuronal loss. Although the strain does not show neuronal loss, we examined *Tg2576* mice, the most widely used AD-model mice carrying the human Swedish APP mutant (60), by means of immunohistochemistry and IP. ASPD-like assemblies were only minimally detected in the cerebral cortex of *Tg2576* mice (supplemental Fig. S7, *A* and *B*);: they were not detected up to 14 months and only a very small amount (~0.01 nmol/mg extracts) was detected at 23 months. As previously reported (18, 61), other Aβ assemblies such as dimers and Aβ*56 were increased in *Tg2576* mice, and total Aβ reached levels comparable with those in human AD (supplemental Fig. S7*C*). With respect to mice with neuronal loss, in addition to certain APP transgenic mice (28, 29), there is a growing number of other AD-model mice, which have been produced by combining APP mutations with either presenilin-1 mutations (62, 63), Tau protein mutations (64), or nitric-oxide synthase knock-out (65). It should be noted that the mouse is not a perfect model of human AD, but these mice are considered to more closely resemble what occurs in the human brains. Therefore, further analysis to examine whether ASPD-like assemblies are present in these mice, which do show massive neuronal loss, will contribute to establish the relationship between neuronal loss and ASPDs.

In addition to the above, we are currently seeking to establish a direct link between native ASPDs and neuronal loss in brains from humans with AD by searching for the toxic target(s) of ASPDs on mature neurons. The identification of native ASPDs and availability of the toxicity-neutralizing antibodies should facilitate a mechanistic understanding of the cellular basis of neuronal cell loss in AD, as well as the development of therapies based on this understanding.

Acknowledgments—We thank Drs. George R. Martin, Takaomi C. Saido, Sangram S. Sisodia, R. Yu, Y. Fukazawa, D. Masui, M. Hoshino, H. Hara, and A. Sakai, for critical discussions; Dr. Charles G. Glabe for providing control blots for A11 antibody through Invitrogen; and Drs. T. Nirasawa, S. Horie, H. Kinoshita, S. Miyama, Y. Ogawa, and N. Takino for technical assistance.

REFERENCES

1. Ross, C. A., and Poirier, M. A. (2005) *Nat. Rev. Mol. Cell Biol.* **6,** 891–898
2. Selkoe, D. J. (1991) *Neuron* **6,** 487–498
3. Lansbury, P. T., and Lashuel, H. A. (2006) *Nature* **443,** 774–779
4. Iwatsubo, T. (2007) *Neuropathology* **27,** 474–478
5. Soto, C., and Estrada, L. D. (2008) *Arch. Neurol.* **65,** 184–189
6. Chiti, F., and Dobson, C. M. (2009) *Nat. Chem. Biol.* **5,** 15–22
7. Hardy, J., and Selkoe, D. J. (2002) *Science* **297,** 353–356
8. Tanzi, R. E., and Bertram, L. (2005) *Cell* **120,** 545–555
9. Saido, T. C., and Iwata, N. (2006) *Neurosci. Res.* **54,** 235–253
10. Klein, W. L., Stine, W. B., Jr., and Teplow, D. B. (2004) *Neurobiol. Aging* **25,** 569–580

11. Walsh, D. M., and Selkoe, D. J. (2007) *J. Neurochem.* **101,** 1172–1184
12. Glabe, C. G. (2008) *J. Biol. Chem.* **283,** 29639–29643
13. Roychaudhuri, R., Yang, M., Hoshi, M. M., and Teplow, D. B. (2009) *J. Biol. Chem.* **284,** 4749–4753
14. Walsh, D. M., Lomakin, A., Benedek, G. B., Condron, M. M., and Teplow, D. B. (1997) *J. Biol. Chem.* **272,** 22364–22372
15. Podlisny, M. B., Ostaszewski, B. L., Squazzo, S. L., Koo, E. H., Rydell, R. E., Teplow, D. B., and Selkoe, D. J. (1995) *J. Biol. Chem.* **270,** 9564–9570
16. Lambert, M. P., Barlow, A. K., Chromy, B. A., Edwards, C., Freed, R., Liosatos, M., Morgan, T. E., Rozovsky, I., Trommer, B., Viola, K. L., Wals, P., Zhang, C., Finch, C. E., Krafft, G. A., and Klein, W. L. (1998) *Proc. Natl. Acad. Sci. U.S.A.* **95,** 6448–6453
17. Barghorn, S., Nimmrich, V., Striebinger, A., Krantz, C., Keller, P., Janson, B., Bahr, M., Schmidt, M., Bitner, R. S., Harlan, J., Barlow, E., Ebert, U., and Hillen, H. (2005) *J. Neurochem.* **95,** 834–847
18. Lesné, S., Koh, M. T., Kotilinek, L., Kayed, R., Glabe, C. G., Yang, A., Gallagher, M., and Ashe, K. H. (2006) *Nature* **440,** 352–357
19. Deshpande, A., Mina, E., Glabe, C., and Busciglio, J. (2006) *J. Neurosci.* **26,** 6011–6018
20. Chimon, S., Shaibat, M. A., Jones, C. R., Calero, D. C., Aizezi, B., and Ishii, Y. (2007) *Nat. Struct. Mol. Biol.* **14,** 1157–1164
21. Lacor, P. N., Buniel, M. C., Chang, L., Fernandez, S. J., Gong, Y., Viola, K. L., Lambert, M. P., Velasco, P. T., Bigio, E. H., Finch, C. E., Krafft, G. A., and Klein, W. L. (2004) *J. Neurosci.* **24,** 10191–10200
22. Kayed, R., Head, E., Thompson, J. L., McIntire, T. M., Milton, S. C., Cotman, C. W., and Glabe, C. G. (2003) *Science* **300,** 486–489
23. Lacor, P. N., Buniel, M. C., Furlow, P. W., Clemente, A. S., Velasco, P. T., Wood, M., Viola, K. L., and Klein, W. L. (2007) *J. Neurosci.* **27,** 796–807
24. Shankar, G. M., Bloodgood, B. L., Townsend, M., Walsh, D. M., Selkoe, D. J., and Sabatini, B. L. (2007) *J. Neurosci.* **27,** 2866–2875
25. Cleary, J. P., Walsh, D. M., Hofmeister, J. J., Shankar, G. M., Kuskowski, M. A., Selkoe, D. J., and Ashe, K. H. (2005) *Nat. Neurosci.* **8,** 79–84
26. Ashe, K. H. (2001) *Learn Mem.* **8,** 301–308
27. Hock, B. J., Jr., and Lamb, B. T. (2001) *Trends Genet.* **17,** S7–S12
28. Calhoun, M. E., Wiederhold, K. H., Abramowski, D., Phinney, A. L., Probst, A., Sturchler-Pierrat, C., Staufenbiel, M., Sommer, B., and Jucker, M. (1998) *Nature* **395,** 755–756
29. Bondolfi, L., Calhoun, M., Ermini, F., Kuhn, H. G., Wiederhold, K. H., Walker, L., Staufenbiel, M., and Jucker, M. (2002) *J. Neurosci.* **22,** 515–522
30. Shankar, G. M., Li, S., Mehta, T. H., Garcia-Munoz, A., Shepardson, N. E., Smith, I., Brett, F. M., Farrell, M. A., Rowan, M. J., Lemere, C. A., Regan, C. M., Walsh, D. M., Sabatini, B. L., and Selkoe, D. J. (2008) *Nat. Med.* **14,** 837–842
31. Kuo, Y. M., Emmerling, M. R., Vigo-Pelfrey, C., Kasunic, T. C., Kirkpatrick, J. B., Murdoch, G. H., Ball, M. J., and Roher, A. E. (1996) *J. Biol. Chem.* **271,** 4077–4081
32. Lue, L. F., Kuo, Y. M., Roher, A. E., Brachova, L., Shen, Y., Sue, L., Beach, T., Kurth, J. H., Rydel, R. E., and Rogers, J. (1999) *Am. J. Pathol.* **155,** 853–862
33. McLean, C. A., Cherny, R. A., Fraser, F. W., Fuller, S. J., Smith, M. J., Beyreuther, K., Bush, A. I., and Masters, C. L. (1999) *Ann. Neurol.* **46,** 860–866
34. Gómez-Isla, T., Hollister, R., West, H., Mui, S., Growdon, J. H., Petersen, R. C., Parisi, J. E., and Hyman, B. T. (1997) *Ann. Neurol.* **41,** 17–24
35. Morrison, J. H., and Hof, P. R. (1997) *Science* **278,** 412–419
36. Larrieu, S., Letenneur, L., Orgogozo, J. M., Fabrigoule, C., Amieva, H., Le Carret, N., Barberger-Gateau, P., and Dartigues, J. F. (2002) *Neurology* **59,** 1594–1599
37. Bouwman, F. H., Schoonenboom, S. N., van der Flier, W. M., van Elk, E. J., Kok, A., Barkhof, F., Blankenstein, M. A., and Scheltens, P. (2007) *Neurobiol. Aging* **28,** 1070–1074
38. Hoshi, M., Sato, M., Matsumoto, S., Noguchi, A., Yasutake, K., Yoshida, N., and Sato, K. (2003) *Proc. Natl. Acad. Sci. U.S.A.* **100,** 6370–6375
39. Lomakin, A., Chung, D. S., Benedek, G. B., Kirschner, D. A., and Teplow, D. B. (1996) *Proc. Natl. Acad. Sci. U.S.A.* **93,** 1125–1129
40. Demuro, A., Mina, E., Kayed, R., Milton, S. C., Parker, I., and Glabe, C. G. (2005) *J. Biol. Chem.* **280,** 17294–17300
41. Kuwano, R., Miyashita, A., Arai, H., Asada, T., Imagawa, M., Shoji, M., Higuchi, S., Urakami, K., Kakita, A., Takahashi, H., Tsukie, T., Toyabe, S., Akazawa, K., Kanazawa, I., and Ihara, Y. (2006) *Hum. Mol. Genet.* **15,** 2170–2182
42. Kayed, R., Head, E., Sarsoza, F., Saing, T., Cotman, C. W., Necula, M., Margol, L., Wu, J., Breydo, L., Thompson, J. L., Rasool, S., Gurlo, T., Butler, P., and Glabe, C. G. (2007) *Mol. Neurodegener.* **2,** 18
43. Mirra, S. S., Heyman, A., McKeel, D., Sumi, S. M., Crain, B. J., Brownlee, L. M., Vogel, F. S., Hughes, J. P., van Belle, G., and Berg, L. (1991) *Neurology* **41,** 479–486
44. Li, Y. T., Woodruff-Pak, D. S., and Trojanowski, J. Q. (1994) *Neurobiol. Aging* **15,** 1–9
45. Kepe, V., Huang, S. C., Small, G. W., Satyamurthy, N., and Barrio, J. R. (2006) *Methods Enzymol.* **412,** 144–160
46. Ince, P. G., and McKeith, I. G. (2003) in *Neurodegeneration: The Molecular Pathology of Dementia and Movement Disorders* (Dickson, D., ed) pp. 188–197, ISN Neuropath Press, Basel
47. Giasson, B. I., Lee, V. M.-Y., and Trojanowski, J. Q. (2004) in *The Neuropathology of Dementia* (Esiri, M., Lee, V. M.-Y., and Trojanowski, J. Q., eds) 2nd Ed., pp. 353–375, Cambridge University Press, Cambridge
48. Kosaka, K. (1990) *J. Neurol.* **237,** 197–204
49. Dezawa, M., Kanno, H., Hoshino, M., Cho, H., Matsumoto, N., Itokazu, Y., Tajima, N., Yamada, H., Sawada, H., Ishikawa, H., Mimura, T., Kitada, M., Suzuki, Y., and Ide, C. (2004) *J. Clin. Invest.* **113,** 1701–1710
50. De Felice, F. G., Velasco, P. T., Lambert, M. P., Viola, K., Fernandez, S. J., Ferreira, S. T., and Klein, W. L. (2007) *J. Biol. Chem.* **282,** 11590–11601
51. Zhao, W. Q., De Felice, F. G., Fernandez, S., Chen, H., Lambert, M. P., Quon, M. J., Krafft, G. A., and Klein, W. L. (2008) *FASEB J.* **22,** 246–260
52. Khosravani, H., Zhang, Y., Tsutsui, S., Hameed, S., Altier, C., Hamid, J., Chen, L., Villemaire, M., Ali, Z., Jirik, F. R., and Zamponi, G. W. (2008) *J. Cell Biol.* **181,** 551–565
53. Laurén, J., Gimbel, D. A., Nygaard, H. B., Gilbert, J. W., and Strittmatter, S. M. (2009) *Nature* **457,** 1128–1132
54. Klein, W. L., Krafft, G. A., and Finch, C. E. (2001) *Trends Neurosci.* **24,** 219–224
55. Bucciantini, M., Giannoni, E., Chiti, F., Baroni, F., Formigli, L., Zurdo, J., Taddei, N., Ramponi, G., Dobson, C. M., and Stefani, M. (2002) *Nature* **416,** 507–511
56. Walsh, D. M., Klyubin, I., Fadeeva, J. V., Cullen, W. K., Anwyl, R., Wolfe, M. S., Rowan, M. J., and Selkoe, D. J. (2002) *Nature* **416,** 535–539
57. Dickson, D. W., and Yen, S. H. (1989) *Neurobiol. Aging* **10,** 402–414
58. Terry, R. D., Masliah, E., Salmon, D. P., Butters, N., DeTeresa, R., Hill, R., Hansen, L. A., and Katzman, R. (1991) *Ann. Neurol.* **30,** 572–580
59. Thal, D. R., Rüb, U., Orantes, M., and Braak, H. (2002) *Neurology* **58,** 1791–1800
60. Hsiao, K., Chapman, P., Nilsen, S., Eckman, C., Harigaya, Y., Younkin, S., Yang, F., and Cole, G. (1996) *Science* **274,** 99–102
61. Kawarabayashi, T., Younkin, L. H., Saido, T. C., Shoji, M., Ashe, K. H., and Younkin, S. G. (2001) *J. Neurosci.* **21,** 372–381
62. Casas, C., Sergeant, N., Itier, J. M., Blanchard, V., Wirths, O., van der Kolk, N., Vingtdeux, V., van de Steeg, E., Ret, G., Canton, T., Drobecq, H., Clark, A., Bonici, B., Delacourte, A., Benavides, J., Schmitz, C., Tremp, G., Bayer, T. A., Benoit, P., and Pradier, L. (2004) *Am. J. Pathol.* **165,** 1289–1300
63. Oakley, H., Cole, S. L., Logan, S., Maus, E., Shao, P., Craft, J., Guillozet-Bongaarts, A., Ohno, M., Disterhoft, J., Van Eldik, L., Berry, R., and Vassar, R. (2006) *J. Neurosci.* **26,** 10129–10140
64. Pérez, M., Ribe, E., Rubio, A., Lim, F., Morán, M. A., Ramos, P. G., Ferrer, I., Isla, M. T., and Avila, J. (2005) *Neuroscience* **130,** 339–347
65. Wilcock, D. M., Gharkholonarehe, N., Van Nostrand, W. E., Davis, J., Vitek, M. P., and Colton, C. A. (2009) *J. Neurosci.* **29,** 7957–7965

Development/Plasticity/Repair

Nurr1 Is Required for Maintenance of Maturing and Adult Midbrain Dopamine Neurons

Banafsheh Kadkhodaei,[1] Takehito Ito,[2] Eliza Joodmardi,[1] Bengt Mattsson,[3] Claude Rouillard,[1] Manolo Carta,[3] Shin-Ichi Muramatsu,[4] Chiho Sumi-Ichinose,[5] Takahide Nomura,[5] Daniel Metzger,[6] Pierre Chambon,[6] Eva Lindqvist,[7] Nils-Göran Larsson,[8,10] Lars Olson,[7] Anders Björklund,[3] Hiroshi Ichinose,[2] and Thomas Perlmann[1,9]

[1]Ludwig Institute for Cancer Research, Stockholm Branch, SE-171 77 Stockholm, Sweden, [2]Graduate School of Bioscience and Biotechnology, Tokyo Institute of Technology, Yokohama 226-8501, Japan, [3]Wallenberg Neuroscience Center, Lund University, SE-221 84 Lund, Sweden, [4]Department of Neurology, Jichi Medical University, Tochigi 329-0498, Japan, [5]Department of Pharmacology, Fujita Health University School of Medicine, Toyoake, Aichi 470-1192, Japan, [6]Department of Functional Genomics Institut de Génétique et Biologie Moléculaire et Cellulaire, 67404 Illkirch, France, Departments of [7]Neuroscience, [8]Laboratory Medicine, and [9]Cell and Molecular Biology, Karolinska Institutet, SE-171 77 Stockholm, Sweden, and [10]Max Planck Institute for Biology of Ageing, D-50931 Cologne, Germany

Transcription factors involved in the specification and differentiation of neurons often continue to be expressed in the adult brain, but remarkably little is known about their late functions. Nurr1, one such transcription factor, is essential for early differentiation of midbrain dopamine (mDA) neurons but continues to be expressed into adulthood. In Parkinson's disease, Nurr1 expression is diminished and mutations in the *Nurr1* gene have been identified in rare cases of disease; however, the significance of these observations remains unclear. Here, a mouse strain for conditional targeting of the *Nurr1* gene was generated, and *Nurr1* was ablated either at late stages of mDA neuron development by crossing with mice carrying Cre under control of the dopamine transporter locus or in the adult brain by transduction of adeno-associated virus Cre-encoding vectors. *Nurr1* deficiency in maturing mDA neurons resulted in rapid loss of striatal DA, loss of mDA neuron markers, and neuron degeneration. In contrast, a more slowly progressing loss of striatal DA and mDA neuron markers was observed after ablation in the adult brain. As in Parkinson's disease, neurons of the substantia nigra compacta were more vulnerable than cells in the ventral tegmental area when *Nurr1* was ablated at late embryogenesis. The results show that developmental pathways play key roles for the maintenance of terminally differentiated neurons and suggest that disrupted function of Nurr1 and other developmental transcription factors may contribute to neurodegenerative disease.

Introduction

Adaptation to a changing environment requires plasticity in the adult CNS. However, to ensure that neurons are properly maintained, such plasticity must be balanced against mechanisms that counteract phenotypic instability. Studies of how neurons develop may help to unravel functions important for the stability of nerve cells as factors promoting their differentiation may also contribute to their maintenance. Indeed, many transcription factors identified for their critical roles during neuronal development continue to be expressed in the postnatal nervous system, raising the possibility that they contribute to the integrity of already differentiated neurons (Hendricks et al., 1999; Vult von Steyern et al., 1999; Kang et al., 2007; Alavian et al., 2008). However, the consequences of adult gene ablation of any of these factors have not yet been reported, and very little is known of their functions in differentiated neurons.

From a clinical perspective, it is of particular interest to identify factors that maintain stability of neurons that are affected in neurodegenerative disorders as loss of phenotype would likely cause or contribute to disease. Parkinson's disease (PD) is characterized by progressive pathology of midbrain dopamine (mDA) neurons of substantia nigra pars compacta (SNc) and the ventral tegmental area (VTA), typically involving deposition of α-synuclein-rich cytoplasmic protein aggregates termed Lewy bodies. During development, early signaling events induce transcription factors that control the specification and differentiation of mDA neurons (Smidt and Burbach, 2007). Several of these factors, including Nurr1, Lmx1a, Lmx1b, Pitx3, FoxA2, and En1/2, continue to be expressed in the postnatal and adult brain (Zetterström et al., 1996; Smidt et al., 1997, 2000; Albéri et al., 2004; Simon et al., 2004; Kittappa et al., 2007). Nurr1, belonging to a family of ligand-independent nuclear receptors (Wang et al.,

Received Aug. 11, 2009; revised Oct. 17, 2009; accepted Oct. 28, 2009.

This work was supported by grants from the Michael J. Fox Foundation (T.P., A.B., L.O.), Vetenskapsrådet via Linné Center DBRM (T.P.), Grants-in-Aid for Human Frontier Science Program (P.C., D.M., H.I.), Grants-in-Aid for Scientific Research from the Ministry of Education, Culture, Sports, Science, and Technology of Japan, the Ministry of Health, Labor, and Welfare of Japan, and the Japan Science and Technology Agency, Core Research for Evolutional Science and Technology (S.-I.M., H.I.), Vetenskapsrådet (L.O.), Swedish Brain Power (L.O.), Swedish Brain Foundation (L.O.), and the Swedish Parkinson Foundatin (L.O.). We are grateful to Johan Ericson and members of the Perlmann and Ericson laboratories for valuable discussions. We thank Andrée Dierich and Jean-Marc Bornert for their help in mouse mutagenesis, Noriko Ihira for help in construction of the targeting vector and screening of ES clones, Björn Anzelius and Naomi Takino for their help with AAV vectors, Ulla Jarl for help with histology, and Marie-Louise Alun for advice on mice handling.

Correspondence should be addressed to either of the following: Thomas Perlmann, Department of Cell and Molecular Biology, Karolinska Institutet, SE-171 77 Stockholm, Sweden, E-mail: thomas.perlmann@licr.ki.se; or Hiroshi Ichinose, Graduate School of Bioscience and Biotechnology, Tokyo Institute of Technology, Yokohama 226-8501, Japan, E-mail: hichinos@bio.titech.ac.jp.

DOI:10.1523/JNEUROSCI.3910-09.2009

 0270-6474/09/2915923-10$15.00/0

2003; Perlmann and Wallén-Mackenzie, 2004), becomes expressed in developing mDA neurons that have just exited the cell cycle and is essential for mDA neuron development because mDA neurons of both the SNc and VTA fail to express dopaminergic markers and newborn *Nurr1*-null mice lack mDA neuron cell bodies and their striatal projections (Zetterström et al., 1997; Castillo et al., 1998; Saucedo-Cardenas et al., 1998). How Nurr1 regulates target genes in mDA neuron development remains essentially unknown but may involve a functional interaction with the homeobox transcription factor Pitx3 (Jacobs et al., 2009).

Determining the role of Nurr1 also in the adult brain is of particular importance because previous studies suggested an association of this protein with PD pathology. Nurr1 expression is diminished in neurons with α-synuclein inclusions in postmortem PD brain tissue, and *Nurr1* mutations and polymorphisms have been identified in rare cases of PD (Xu et al., 2002; Le et al., 2003; Zheng et al., 2003; Grimes et al., 2006). However, the significance of genetic lesions remain unclear (Wellenbrock et al., 2003; Hering et al., 2004; Tan et al., 2004). These observations emphasize the importance of elucidating the role of Nurr1 in more mature mDA neurons by analyzing the consequences of conditional *Nurr1* gene ablation in mice.

Materials and Methods

Conditional Nurr1 gene-targeted mice. Mouse 129SV genomic library constructed in bacterial artificial chromosome (BAC) was screened by PCR. A BAC clone containing the entire Nurr1 gene was selected, and a BamHI–MunI fragment containing exon 1 to exon 5 was recloned into a pBluescript II vector. A floxed neomycin cassette was inserted into an internal EcoRI site located in intron 3, and a synthetic loxP sequence was inserted at SalI site located in intron 2. Mouse embryonic stem (ES) cells were electroporated with the targeting vector, and the homologously recombinated clones were screened by PCR and Southern blot analysis. ES clones with three loxP sites were selected, and a plasmid expressing Cre DNA recombinase was transiently transfected into the cells. ES cells with two loxP sites without a neomycin cassette were selected by PCR and used for production of chimeric mice.

Animals. Mice were kept in rooms with controlled 12 h light/dark cycles, temperature, and humidity, with food and water provided *ad libitum*. All animal experiments were performed with permission from the local animal ethics committee. The generation of dopamine transporter (*DAT*)–*Cre* mutant mice has been described previously (Ekstrand et al., 2007). Mice were mated during the night, and the females were checked for vaginal plugs in the morning [day of vaginal plug considered as embryonic day 0.5 (E0.5)].

L-3,4-Dihydroxyphenylalanine treatment. Methyl L-3,4-dihydroxyphenylalanine (L-DOPA) hydrochloride and the peripheral DOPA decarboxylase inhibitor benserazide-HCl (Sigma-Aldrich) were dissolved in Ringer's solution immediately before use. L-DOPA was intraperitoneally given every second day at the dose of 2.5 mg/kg combined with 0.625 mg/kg benserazide. Chronic treatment with L-DOPA/benserazide was administered for 50 d, starting at postnatal day 15 (P15). During this period, the mice were carefully observed and weight was measured regularly. Reported hyperactivity was observed in $cNurr1^{DATCre}$ mice when given a single higher dose of L-DOPA (25 mg/kg L-DOPA, 6.25 mg/kg benserazide).

Histological analyses. At embryo stages, embryos were fixed for 2–24 h in 4% phosphate-buffered paraformaldehyde (PFA), cryopreserved in 30% sucrose before being embedded in OCI (Sakura Finetek), and cryosectioned at a thickness of 10–20 μm onto slides (SuperFrostPlus; Menzel Gläser). For the isolation of brains for immunolabeling at P15 and onward, animals were anesthetized with Avertin (tribromoethanol; 0.5 mg/g) and perfused through the left ventricle with body-temperature PBS, followed by ice-cold 4% PFA. The brains were dissected and post-fixed overnight in 4% paraformaldehyde and subsequently cryoprotected for 24–48 h in 30% sucrose at 4°C. The brains were serially sectioned on a cryostat or sliding microtome at 10–30 μm. Littermates were used in an all comparative experiments.

For immunohistochemistry, sections were preincubated for 1 h in blocking solution containing either 10% normal goat sera or 5–10% bovine serum albumin, 0.25% Triton X-100, and 0.01% Na-azide in PBS. Primary antibodies diluted in blocking solution were applied overnight at 4°C. After rinses with PBS, biotinylated- or fluorophore-conjugated secondary antibodies diluted in PBS were applied for 1 h at room temperature. Biotinylated secondary antibodies were followed by incubation with streptavidin–horseradish peroxidase complex (ABC elite kit, Vectastain) for 1 h and subsequent exposure to diaminobenzidine (DAB kit; Vector Laboratories). Primary antibodies and dilution factors were as follows: rabbit anti-Nurr1 (1:100; M196; Santa Cruz Biotechnology), anti-Nurr1 (1:250; E20; Santa Cruz Biotechnology), rabbit anti-tyrosine hydroxylase (TH) (1:500; Pel-Freeze), rat anti-DAT (1:2000; Millipore Bioscience Research Reagents), mouse anti-TH (1:200; Millipore Bioscience Research Reagents), rabbit anti-vesicular monoamine transporter (VMAT) (1:500; Millipore Bioscience Research Reagents), rabbit anti-L-DOPA decarboxylase (AADC) (1:500; Millipore Bioscience Research Reagents), rabbit anti-Cre (1:10,000; Covance Research Products), guinea pig anti-Lmx1b (1:1000) (Andersson et al., 2006), and rabbit anti-Pitx3 (Smidt et al., 2004). In some cases (anti-AADC, anti-VMAT, and anti-Nurr1), the blocking steps were performed after antigen retrieval (Dako). Finally, expression was detected by secondary antibodies from Jackson ImmunoResearch. Section images were collected by confocal microscopy (Leica DMIRE2) and bright-field microscopy (Eclipse E1000K; Nikon). Cell counting was performed by counting all SNc DA neurons detected by immunohistochemistry (DAB) in a total of three sections per animal (every 12th tissue section) within the ventral midbrain of animals taken at 4 months after vector injection in both wild-type wt^{AAVCre} and $cNurr1^{AAVCre}$ animals. The mean of counted cells per animal was established from both the injected and non-injected sides in each animal, and the relative decrease was calculated as a percentage as described in Results.

AAV–Cre injections. Two and a half- to 5-month-old animals received one unilateral stereotaxic injection in the right striatum using a 10 μl Hamilton microsyringe fitted with a glass pipette tip. The animals were anesthetized with isoflurane, 1 μl was injected during 5 min, and the cannula was left in place for an additional 2 min before being slowly retracted. The anteroposterior and mediolateral coordinates from bregma were −2.8 and −1.1 mm, respectively, and the dorsoventral coordinates from the dura were −4.3 mm. Animals were killed 0.5, 1.5, and 4 months after injection, and the brains were isolated.

Measurement of tissue content for dopamine, serotonin, and their metabolites. In supplemental Tables 1–3 (available at www.jneurosci.org as supplemental material), tissues were collected from P1, P7, P14, and adult (P48) wt^{DATCre} and $cNurr1^{DATCre}$ mice. One- to 14-d-old mice were killed by decapitation, and P48 mice were killed by cervical dislocation. Brains were rapidly removed, chilled in saline (4°C), dissected, frozen on dry ice, and stored at −80°C until use. To process tissues for HPLC and electrochemical detection of monoamines and metabolites, samples were homogenized by sonication in 5 vol or in 30 μl of 0.1 M perchloric acid, followed by centrifugation. Endogenous levels of noradrenaline, DA, 3,4-dihydroxyphenylacetic acid, homovanillic acid (HVA), serotonin (5-HT), and 5-hydroxyindoleacetic acid were determined in the supernatants. A reverse column (BAS, C-18, 100.0 × 3.2 mm, 3 μm particle diameter) was used for separation. The mobile phase consisted of 0.05 M sodium phosphate/0.03 M citric acid buffer containing 0.1 mM EDTA and was adjusted with various amounts of methanol and sodium-L-octane sulfonic acid. The flow rate was 0.3 ml/min. Monoamines and metabolites were detected using a glassy-carbon electrode detector, which as set at +0.7 V versus an Ag/AgCl reference electrode. Resultant peaks were measured and compared with repeated control samples containing fixed mixed amounts of compounds of interest.

In supplemental Table 4 (available at www.jneurosci.org as supplemental material), all animals were killed, and striata and cortex were rapidly dissected out, frozen on dry ice, and stored at −80°C. To determine monoamines, tissue was homogenized in 0.1 M perchloric acid and centrifuged at 10,000 rpm for 10 min before filtering though minispin filters for an additional 3 min at 10,000 rpm. The tissue extract were then analyzed by HPLC as described previously (Carta et al., 2007) with minor

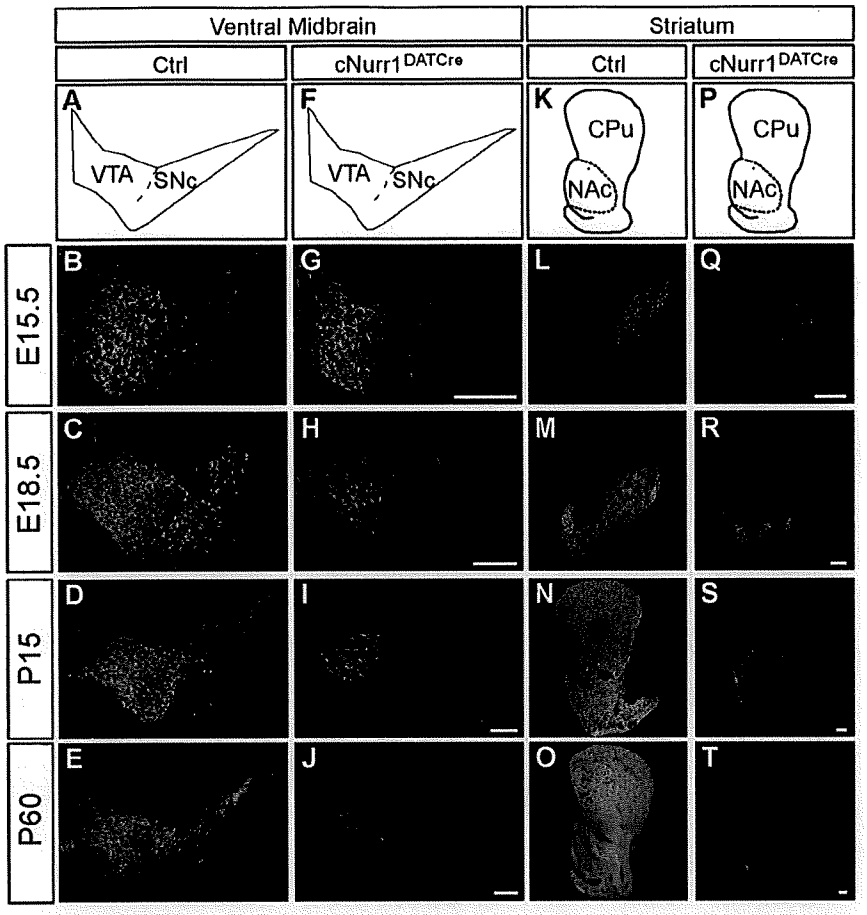

Figure 1. TH is progressively lost in both the ventral midbrain and striatum of *cNurr1*^{DATCre} mice. ***A–T***, Confocal microscopy showing TH immunohistochemistry in control (ctrl) and *cNurr1*^{DATCre} mice as indicated. ***A–J***, Sections were analyzed at the levels of ventral midbrain (as indicated in ***A*** and ***F***) and in the striatum (as indicated in ***K*** and ***P***). TH immunofluorescence was analyzed at both embryonal and postnatal stages as indicated. Results demonstrate a progressive loss of TH immunoreactivity in the ventral midbrain. Note that TH immunoreactivity was more drastically downregulated at more lateral regions compared with the prospective medial VTA. ***K–T***, TH immunoreactivity in the striatum. In *cNurr1*^{DATCre} mice, TH was lost in the CPu and diminished in the NAc. Scale bars, 250 μm.

modifications. Briefly, 25 μl of each sample were injected by a cooled autosampler (Midas) into an ESA Coulochem III coupled with an electrochemical detector. The mobile phase (5 g/L sodium acetate, 30 mg/L Na2-EDTA, 100 mg/L octane-sulfonic acid, and 10% methanol, pH 4.2) was delivered at a flow rate of 500 μl/min to a reverse-phase C18 column (4.6 mm diameter, 150 mm).

Fluorogold retrograde tracing. Animals received one unilateral stereotaxic injection in the right striatum using a 5 μl Hamilton microsyringe (22 gauge steel cannula) filled with the retrograde tracer Fluorogold (hydroxystilbamidine, 4%, Biotium). The animals were anesthetized with isoflurane, 0.5 μl was injected during 1 min, and the cannula was left in place for an additional 2 min before slowly being retracted. The anteroposterior and mediolateral coordinates from bregma were 0.27 and −2.10 mm, respectively, and the dorsoventral coordinates from the dura were −2.60 mm. Animals were killed 4 d after injection, and the brains were isolated. Fresh-frozen sections (14 μm) were cut with a cryostat and examined under a epifluorescence microscope (Eclipse E1000K; Nikon) coupled to an RTke spot camera.

Open-field test. This test was used to monitor overall activity and rearing behavior. The open field consisted of a white plastic box (55 × 35 × 30 cm) with lines (squares of 7 × 35 cm) painted on its floor. The animals were put in the center of the box, habituated for 10 min, and filmed 15 min thereafter while rearing was scored. The video recordings were used to measure the number of lines crossed during the monitoring period. A line crossing was counted when the mouse moved its whole body from one square to another.

Stepping test. Forelimb akinesia was monitored in a modified version of the stepping test, as described previously for rats (Schallert et al., 1992; Kirik et al., 1998). The test was performed three times daily over 3 consecutive days. In this test, the mouse was held firmly by the experimenter with both hindlimbs and one forelimb immobilized, and the mouse was passively moved with the free limb contacting a table surface. The number of adjusting steps, performed by the free forelimb when moved in the forehand and backhand directions, over a distance of 30 cm, was recorded. Results are presented as data collected on the third testing day.

Results

Selective *Nurr1* ablation in late developing mDA neurons

A mouse strain containing a *Nurr1* allele for conditional gene ablation was generated by insertion of two loxP sequences in the second and third introns so that the coding sequence, including the first coding exon 3, is excised by Cre-mediated recombination (supplemental Fig. 1, available at www.jneurosci.org as supplemental material). To analyze the consequences of *Nurr1* ablation at late stages of mDA neuron development, we crossed floxed *Nurr1* mice with mice carrying *Cre* inserted in the locus of the *DAT* gene (Ekstrand et al., 2007). Crosses generated *Nurr1* mice that were homozygous for the conditional targeted *Nurr1* allele and heterozygous for the *DAT–Cre* allele ($Nurr1^{L2/L2};DAT^{Cre/wt}$; hereafter referred to as *cNurr1*^{DATCre} mice). Littermates of genotype $Nurr1^{L2/L2}$; $DAT^{wt/wt}$ or $Nurr1^{w/w};DAT^{Cre/wt}$ were used as controls. Although we cannot exclude that a small number of cells escape Nurr1 gene deletion, immunohistochemistry using an antibody against Nurr1 showed that *DAT–Cre*-mediated *Nurr1* ablation resulted in the expected delayed loss of Nurr1 expression in mDA neurons beginning from approximately E13.5 and becomes essentially complete at E15.5 (supplemental Fig. 2, available at www.jneurosci.org as supplemental material). At this stage of normal development, cells express pan-neuronal properties as well as many mDA neuron markers, and axons are growing toward the developing striatum (Smidt and Burbach, 2007).

cNurr1^{DATCre} mice were born at the expected Mendelian frequency of ~25% (of a total $n = 159$); however, *cNurr1*^{DATCre} mice were less active than controls and did not survive beyond 3 weeks after birth. If litters were allowed to remain with their mothers after weaning, perinatal death was avoided in ~50% of *cNurr1*^{DATCre} pups. These surviving mice were, however, ~40% smaller than controls at the age of 2 months (supplemental Fig. 3, available at www.jneurosci.org as supplemental material). Although no significant change in spontaneous light-phase locomotor activity could be observed in adult *cNurr1*^{DATCre} mice, rearing was dramatically decreased (supplemental Fig. 3, avail-

able at www.jneurosci.org as supplemental material). L-DOPA treatment of mutant mice did not improve viability and did not induce any weight gain. Instead, *cNurr1*^{DATCre} mice display a pronounced and severe hypersensitivity to L-DOPA treatment characterized by an acute phase of hyperactivity and repetitive behaviors (including repetitive gnawing, excessive grooming, and self-injury) in all tested mutant ($n = 9$) but not in any wild-type controls ($n = 7$) (see Materials and Methods). These behaviors resemble those that have been observed in neonatal 6-hydoxydopadmine lesioned rats treated with L-DOPA (Breese et al., 2005). In conclusion, late embryonic mDA neuron-selective *Nurr1* ablation is associated with decreased weight, rearing, and viability, and mice show an altered response to L-DOPA.

Reduced levels of TH and DA in brains of *cNurr1*^{DATCre} mice

The observed abnormalities are consistent with a dopaminergic deficiency. To analyze the possible cellular basis for the phenotype, brain sections from controls and *cNurr1*^{DATCre} mice were analyzed by immunohistochemistry using an antibody against TH (Fig. 1). A progressive loss of TH immunostaining in SNc was observed in the *cNurr1*^{DATCre} mice (Fig. 1*A–J*). TH levels were significantly decreased already at E15.5, soon after Nurr1 is lost, and decreased further until adulthood when only scattered TH-positive neurons could be detected. TH was diminished also within the VTA at later stages, but a significant number of cells remained even in adult animals (Fig. 1*A–J*). These cells were counted in four nonconsecutive sections for each analyzed brain. In adult control VTA, a mean of 74.5 ± 7.1 cells per section were counted in *cNurr1*^{DATCre} mice ($n = 4$) and 499.3 ± 5.2 cells in controls ($n = 3$) (Student's t test, 4.4×10^{-7}). TH immunostaining within the caudatus putamen (CPu) was completely lost (Fig. 1*K–T*). However, weak immunoreactivity remained in nucleus accumbens (NAc) innervated preferentially by VTA neurons (Fig. 1*K–T*). We also noted the appearance of ectopic TH-positive cell bodies within the striatal parenchyma in *cNurr1*^{DATCre} mice (supplemental Fig. 4, available at www.jneurosci.org as supplemental material). These cells were more frequent in regions in which striatal TH had been most severely depleted as a consequence of Nurr1 ablation and resemble TH-positive neurons appearing in rodent and primate DA-depletion models (Huot and Parent, 2007). Decreased levels of TH immunostaining were paralleled by decreased DA levels, as measured by HPLC (supplemental Tables 1–3, available at www.jneurosci.org as supplemental material). Striatal DA was dramatically reduced to 14% of controls at P1 in *cNurr1*^{DATCre} mice and was almost completely lost by P60. An increased ratio of HVA to DA at P14 indicated increased turnover of DA in remaining cells at this stage (supplemental Table 2, available at www.jneurosci.org as supplemental material). DA was more severely decreased in CPu compared with NAc (supplemental Table 3, available at www.jneurosci.org as supplemental material). In contrast, 5-HT was significantly increased in both CPu and NAc, consistent with previous findings showing increased serotonergic innervation after striatal DA depletion (Snyder et al., 1986). Thus, a severe neurotransmitter deficiency of the mesostriatal DA system is apparent in *cNurr1*^{DATCre} mice. Together, measurements of TH immunoreactivity and DA levels demonstrate that Nurr1 is critically required for maintaining TH expression and DA synthesis from late stages of mDA neuron differentiation.

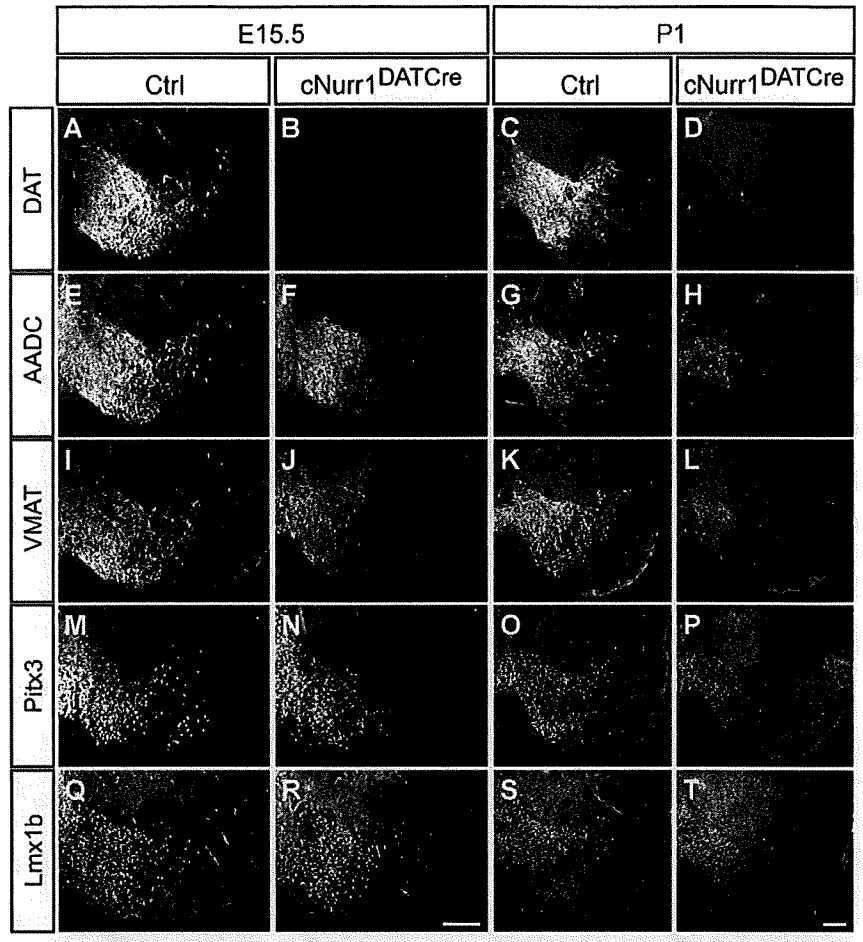

Figure 2. All analyzed mDA neuron markers are lost or diminished in *cNurr1*^{DATCre} mice. ***A–T***, Confocal microscopy showing immunohistochemistry of several different mDA neuron markers in control (ctrl) and in *cNurr1*^{DATCre} mice at E15.5 or at P1, as indicated. The following markers were analyzed: DAT, AADC, VMAT, Pitx3, and Lmx1b. Results show a progressive loss of markers that is more substantial in the lateral SNc, whereas more medial VTA cells are lost more slowly. DAT is completely absent already at E15.5 in *cNurr1*^{DATCre} mice, whereas all other markers are decreased more slowly in this area (compare ***A***, ***B***). Scale bars, 200 μm.

Cellular deficiency within the ventral midbrain of *cNurr1*^{DATCre} mice

To investigate whether the phenotype is a consequence of a more limited disruption of DA synthesis or a more severe cellular deficiency, a number of additional mDA neuron markers were analyzed. All analyzed mDA neuron markers were diminished or absent within SNc in *cNurr1*^{DATCre} mice already at E15.5 (Fig. 2). DAT was completely lost at E15.5 and therefore, consistent with previous data (Sacchetti et al., 1999), stands out as being a likely direct target of Nurr1 (Fig. 2*A–D*). Additional control experiments showed that DAT and other markers, including TH and

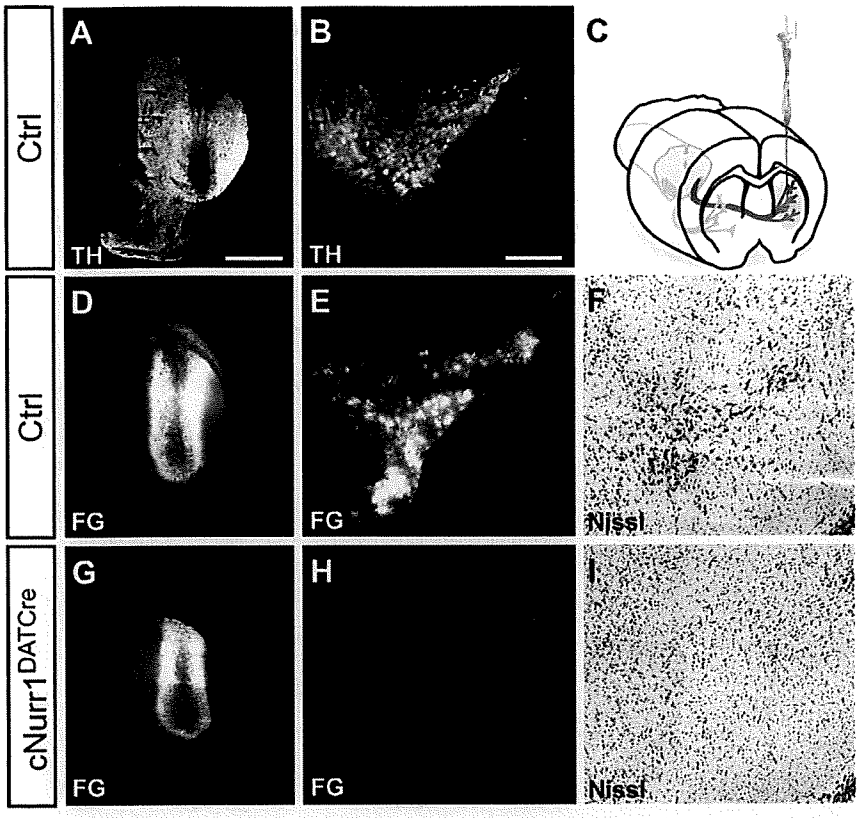

Figure 3. Cell bodies and striatal innervation are lost in $cNurr1^{DATCre}$ mice as determined by Fluorogold (FG) retrograde tracing of fibers extending from cell bodies in SNc to the striatum. ***A–C***, After Fluorogold injection, injected into the left striatum in either adult (1.5 months old) control (Ctrl) or $cNurr1^{DATCre}$ mice as indicated in ***C***, mice were killed after 4 d and analyzed for TH immunofluorescence in the striatum (***A***) or ventral midbrain (***B***). ***D–I***, Analysis for Fluorogold (FG) or by Nissl staining. Strong Fluorogold staining in both striatum (***D***) and in the ventral midbrain (***E***) was consistently seen in all control (Ctrl) animals ($n = 7$). In contrast, Fluorogold fluorescence was only detected in the striatum (***G***) in $cNurr1^{DATCre}$ mice ($n = 5$), indicating that fibers from the SNc (***H***) had been lost in these animals. Moreover, large, densely packed cell bodies are only visualized by Nissl staining in the ventral midbrain of control animals (***F***) but are completely absent from $cNurr1^{DATCre}$ mice (***I***). Striatal site of Fluorogold injection is marked by asterisk in ***A***, ***D***, and ***G***. Scale bars: ***A***, ***B***, ***D***, ***E***, ***G***, ***H***, 1 μm; ***F***, ***I***, 1200 μm.

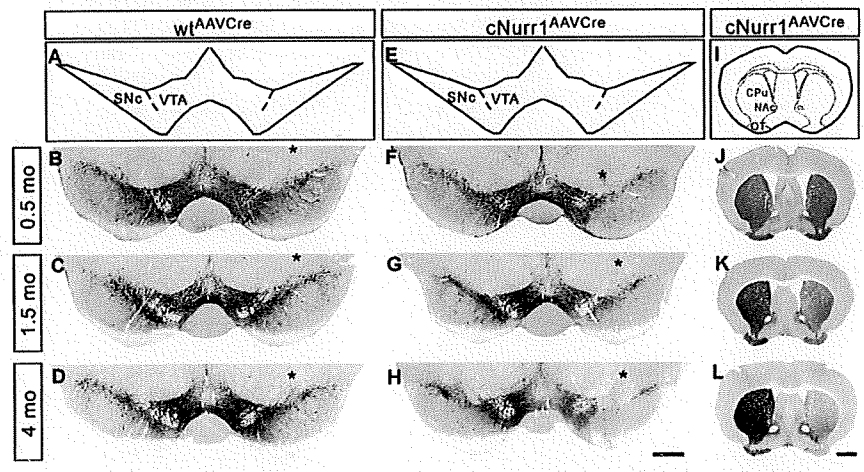

Figure 4. TH expression in both the ventral midbrain and striatum is progressively lost in the injected, but not non-injected, side of $cNurr1^{AAVCre}$ mice. ***A–H***, Sections from 0.5, 1.5, and 4 month (mo; as indicated) old AAV–Cre-injected controls (wt^{AAVCre}) or $cNurr1^{AAVCre}$ mice were used for analyses by nonfluorescent DAB TH immunostaining in the ventral midbrain. The analyzed region within the ventral midbrain is schematically illustrated in ***A*** and ***E***. The site of injection, marked by an asterisk in ***B–D*** and ***F–H***, was verified in all animals by high-power magnification microscopy and was identified as a small area of injection-induced necrosis. Results show that TH immunostaining is not drastically altered at 0.5 months but is progressively decreased at 1.5 and 4 months in the injected SNc and VTA. ***I–L***, DAB TH staining at the level of striatum. Analyzed regions are indicated in ***I***. TH staining is progressively decreased at 1.5 and 4 months in the side that is ipsilateral to the side of AAV–Cre injection in $cNurr1^{AAVCre}$ mice (***J–L***). OT, Olfactory tubercle. Scale bars: ***A–H***, 600 μm; ***I–L***, 1 mm.

Nurr1, were not visibly decreased in mice heterozygous for the *DAT–Cre* allele (supplemental Fig. 5, available at www.jneurosci.org as supplemental material) (data not shown). In contrast to DAT, AADC, VMAT2, Pitx3, or Lmx1b were not reduced within the most medial ventral midbrain at this early stage and, with the exception of DAT, markers were not completely downregulated at P1 (Fig. 2*E–T*). The progressive loss of markers indicates a severe loss of phenotype within the SNc, whereas cells within the VTA appear more resilient. Importantly, most TH-positive cells within the VTA have lost any detectable expression of DAT, indicating that these cells have not escaped Nurr1 gene targeting (supplemental Fig. 6, available at www.jneurosci.org as supplemental material).

To further assess the extent of a cellular deficiency, striatal target innervation was analyzed by Fluorogold retrograde tracing after injection into the striatum of live 8- to 9-week-old controls and $cNurr1^{DATCre}$ mice. Fluorogold was transported into SNc cell bodies of control mice; however, fluorescence was entirely undetected within the SNc of Fluorogold-injected $cNurr1^{DATCre}$ mice (Fig. 3, compare *D*, *E* with *G*, *H*). In addition, characteristic large and densely packed TH-immunoreactive mDA neurons within the SNc were virtually absent in $cNurr1^{DATCre}$ mice (Fig. 3*I*). In conclusion, Nurr1 ablation in $cNurr1^{DATCre}$ mice results in rapid loss of SNc cell bodies; however, scattered VTA neurons remained even in adult $cNurr1^{DATCre}$ mice.

Adeno-associated virus–Cre-mediated *Nurr1* ablation in adult mice

In $cNurr1^{DATCre}$ mice, *Nurr1* is ablated well before full mDA neuron maturity and before targets in the striatum have become innervated; thus, it remained possible that the phenotype is a consequence of a developmental dysfunction. Therefore, we proceeded to inactivate *Nurr1* specifically in ventral midbrain of adult mice, using an adeno-associated virus (AAV)–Cre vector driven by the neuron-specific synapsin promoter. AAV–Cre was administered by unilateral stereotaxic microinjection above the right SNc. Cre immunohistochemistry and β-galactosidase expression was analyzed after intranigral AAV–Cre injection into reporter mice in which the ROSA26 locus is targeted with a LacZ reporter gene (Soriano, 1999). Results show widespread Cre expression around the site of injection, spreading into both SNc and VTA, and robust recombination of the LacZ reporter construct (supplemental Fig. 7, available at www.jneurosci.org as supple-

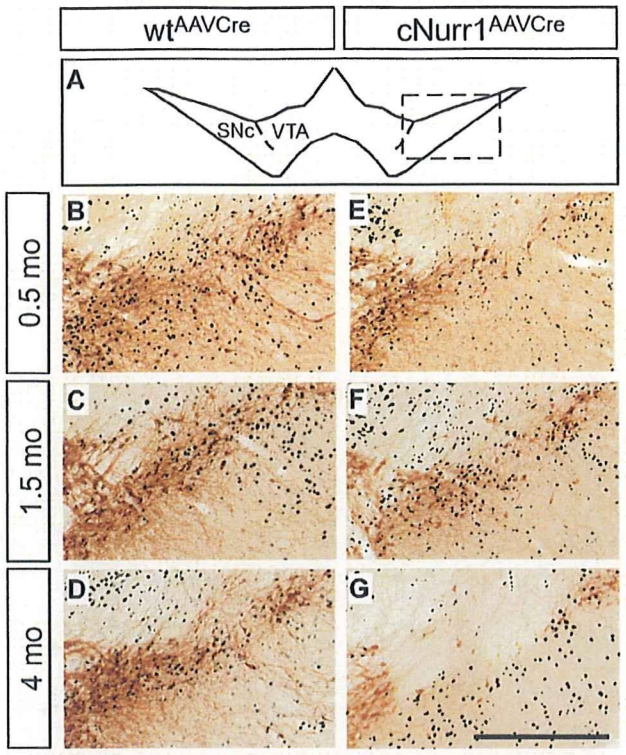

Figure 5. Cre-expressing cells are lost at 4 months within the SNc after Nurr1 ablation. *A*, Higher magnification showing TH by DAB staining (brown) at the level of the injected SNc in wt^{AAVCre} and $cNurr1^{AAVCre}$ mice. The region that has been magnified is boxed in *A*. *B–G*, Adjacent sections were immunostained for Cre (black) and are superimposed on the DAB-stained TH sections in all micrographs. Cre staining is widespread in the area in which mDA neurons are normally localized at 0.5 and 1.5 months (*E*, *F*) but almost completely absent in this area at 4 months (*G*). Scale bar, 500 μm.

mental material). Moreover, except for a small necrotic area around the site of injection, virus administration did not affect tissue morphology, expression of mDA neuron markers, or microglia activation (data not shown).

AAV–Cre was unilaterally injected above the SNc of adult mice homozygous for the floxed *Nurr1* allele to generate adult conditional gene-targeted mice ($cNurr1^{AAVCre}$) or into wild-type control mice (wt^{AAVCre}). In addition, a vector encoding the green fluorescent protein (GFP) driven by the synapsin promoter (AAV–GFP) was injected in mice homozygous for the floxed *Nurr1* allele ($cNurr1^{AAV-GFP}$ mice) to ensure that the floxed animals are not more sensitive to nonspecific toxicity induced by AAV transduction. Histological analyses were performed from animals killed at 0.5, 1.5, and 4 months after injection.

Reduction of TH and DA in adult *Nurr1*-ablated mice

TH immunohistochemistry at the level of the ventral midbrain was analyzed to assess the consequences of adult *Nurr1* ablation. Within SNc, TH immunoreactivity was unaffected at 0.5 months but was progressively reduced at 1.5 and 4 months in the injected SNc in $cNurr1^{AAVCre}$ mice (Fig. 4*E–H*). In contrast, TH immunoreactivity was unaffected in SNc of control wt^{AAVCre} and $cNurr1^{AAV-GFP}$ mice (Fig. 4*A–D*) (data not shown). TH was also reduced in the VTA at 1.5 and 4 months; however, at 4 months, the reduction in VTA was less dramatic compared with SNc (Fig. 4*E–H*).

Decreased striatal TH immunoreactivity paralleled the reduction in the ventral midbrain. Thus, although no signs of degenerating striatal TH-stained fibers (swollen axons or dystrophic neurites) were detected, striatal sections ipsilateral to the side of AAV–Cre injection showed clearly reduced TH in $cNurr1^{AAVCre}$ mice but not in controls (wt^{AAVCre} or $cNurr1^{AAV-GFP}$) (Fig. 4*I–L*) (supplemental Fig. 8, available at www.jneurosci.org as supplemental material). Diminished TH immunoreactivity was observed in regions innervated by both SNc and VTA (CPu and NAc, respectively), consistent with the reduced TH immunoreactivity in both SNc and VTA mDA neuron cell bodies. Measurement of DA and metabolites by HPLC from dissected tissue at 4 months confirmed this picture as a significant reduction in DA and DA metabolites noted both within the dorsolateral striatum and in areas mostly innervated by the VTA (cortex and ventromedial striatum) (supplemental Table 4, available at www.jneurosci.org as supplemental material). Thus, TH, DA, and DA metabolites are clearly reduced as a result of adult *Nurr1* ablation.

Loss of mDA neuron characteristics in adult *Nurr1*-ablated mice

To further analyze the fate of *Nurr1*-ablated neurons, cells were counted within the SNc and VTA in $cNurr1^{AAVCre}$ and wt^{AAVCre} mice. Within SNc, the number of TH-positive cells was significantly decreased at 4 months (58.1 ± 8.3 and 95.4 ± 6.3% in the injected vs non-injected sides of $cNurr1^{AAVCre}$ and wt^{AAVCre} mice, respectively; $p = 0.0053$). In contrast, the numbers of TH-positive cells was not significantly reduced within the VTA (104.1 ± 4.7 and 101.6 ± 10.5% in the injected versus non-injected sides of $cNurr1^{AAVCre}$ and wt^{AAVCre} mice, respectively). Also, the numbers of TH-positive cells were not significantly changed in $cNurr1^{AAVCre}$ mice at 1.5 months (data not shown).

To assess the integrity of neurons, cellular analysis was extended by analyzing Cre-immunolabeled sections that were superimposed on adjacent TH-labeled sections (Fig. 5). Notably, in $cNurr1^{AAVCre}$ mice, Cre expression was clearly detected within the area of SNc at both 0.5 and 1.5 months but was lost at 4 months in the region in which mDA neurons should normally be localized (Fig. 5, compare *E–G* with *B–D*). Cre expression is driven by a general neuronal promoter (synapsin), suggesting that loss of Nurr1 may eventually affect some pan-neuronal properties at 4 months after ablation.

Confocal microscopy confirmed the loss of TH at 1.5 and 4 months after Nurr1 ablation and the loss of Cre at 4 months (Fig. 6*A–D*). At 1.5 months, DAT expression was weak but cell bodies were readily identified (Fig. 6*E*,*F* and inset in *F*). DAT staining remained also at 4 months, but, at this stage, high-power magnification indicated that some of the staining appeared confined to fibers and/or dystrophic cells (Fig. 6*G*,*H* and inset in *H*). Nonetheless, at 4 months, most cells with decreased TH stained positive for AADC, showing that not all mDA neuron characteristics were affected (Fig. 7*A–F*). Moreover, VMAT2 is yet another marker that was severely decreased in $cNurr1^{AAVCre}$ mice, but remaining weakly stained cells were positive for the general neuronal marker Hu (Fig. 7*G–L*). The observed changes were not correlated to increased number of apoptotic cells because increased activated Caspase 3 could not be detected (data not shown). Also, we found no evidence for nigral inflammation or α-synucleinopathy because activated microglia and α-synuclein-rich inclusions were not detected at any stage after Nurr1 ablation in $cNurr1^{DATCre}$ mice (data not shown). Finally, TH and DAT expression in VTA was also affected, without any apparent loss of the neuronal marker Hu or any signs of dystrophic cells (supplemental Fig. 9, available at www.jneurosci.org as supplemental material) (data not shown). Thus, Nurr1 ablation results in a

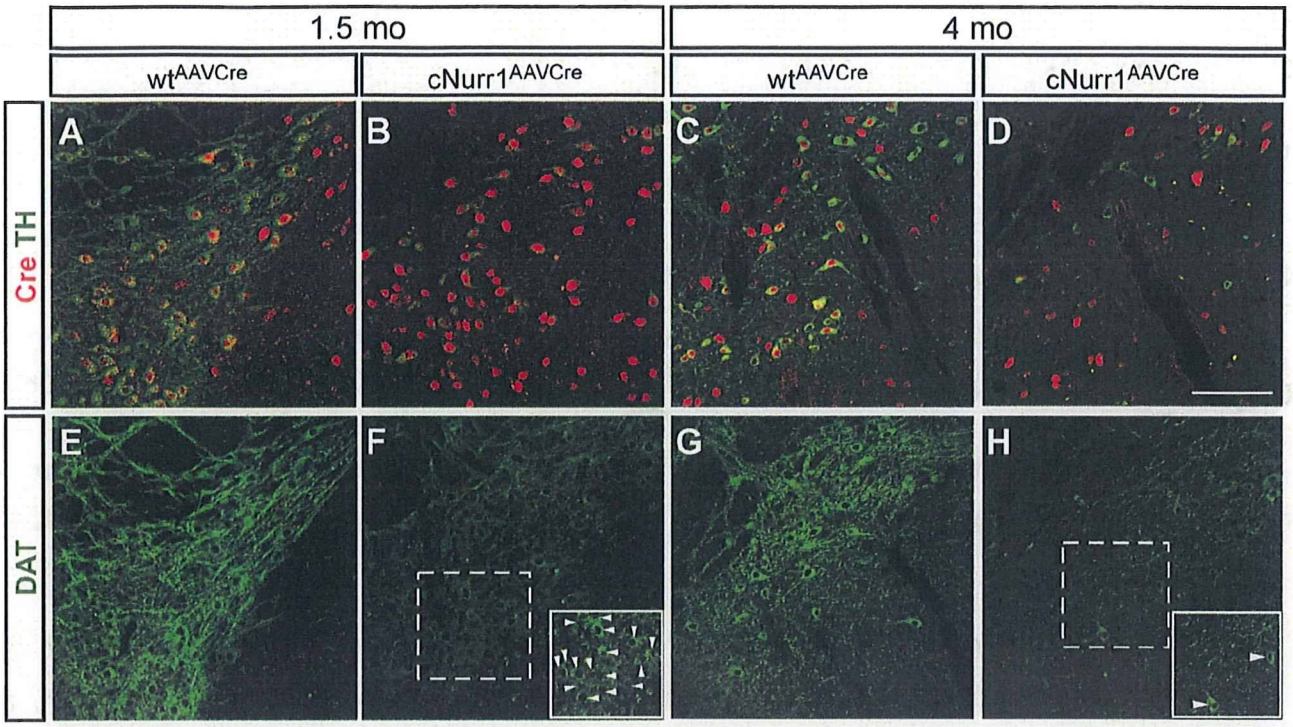

Figure 6. Decreased expression of DAT and signs of dystrophic cells in $cNurr1^{AAVCre}$ mice. ***A–H***, Confocal analysis of SNc in wt^{AAVCre} and $cNurr1^{AAVCre}$ mice at 1.5 and 4 months, as indicated. Confocal images show double staining of Cre (red) and TH (green; ***A–D***) and staining for DAT (green; ***E–H***). Micrographs show that there is a loss of TH and DAT and a progressive loss of synapsin-driven Cre at 4 months. At 4 months, DAT staining appears fragmented and stains scattered fibers, whereas very few intact cell profiles (marked with arrowheads in ***F*** and ***H***) can be identified in $cNurr1^{AAVCre}$ mice (compare insets in ***F***, ***H***). Scale bar, 200 μm.

progressive dysfunction characterized by a partial loss of the mDA neuron phenotype. Although we see few signs of neuronal degeneration, we cannot exclude a limited cell loss.

To assess whether the observed dysfunction was paralleled by an altered motor behavior, $cNurr1^{AAVCre}$ mice were subjected to a stepping test at 3 and 4 months (Schallert et al., 1992; Kirik et al., 1998). Performance of the left forelimb (i.e., the limb contralateral to the vector injection) was impaired at both time points (Fig. 8). Additional behavioral testing, including amphetamine-induced rotations and a corridor test, indicated that individual mutant animals appeared affected; however, the *Nurr1*-ablated group did not show alterations that were statistically significant (supplemental Fig. 10, available at www.jneurosci.org as supplemental material). Our results demonstrate progressive mDA neuron dysfunction, leading to a more severe deficiency at 3–4 months after *Nurr1* ablation.

Discussion

This study provides definitive evidence that Nurr1 is not only critical for early differentiation but also for the maintenance of functional mDA neurons. Conditional gene targeting at late embryogenesis, when characteristic features of mDA neurons are already apparent, results in a rapid and close to complete mDA neuron loss. Only few TH-positive cells remain within the VTA also in the absence of Nurr1. Removal of Nurr1 leads to a severe dysfunction also in adult mDA neurons. It should be noted that reduction of striatal DA and the behavioral effects after adult ablation most likely underestimate the importance of Nurr1 in the adult brain because AAV injection only transduced a proportion of all mDA neurons in the injected side of treated animals. Thus, these data emphasize the importance of studying developmental mechanisms for elucidating neuron maintenance mechanisms. An analogous example is provided by the glial cell line-derived neurotrophic factor (GDNF). GDNF is known to promote neuronal survival under development, but only recently has conditional gene targeting enabled studies that interrogate the role of GDNF and other factors signaling via Ret for maintenance of midbrain dopamine neurons in the adult brain (Oo et al., 2003; Jain et al., 2006; Kramer et al., 2007; Pascual et al., 2008).

Data presented here have implications for our understanding of how mature differentiated cell types are maintained. Previous studies have indicated that the differentiated state is not irreversible because even mature specialized cells, including for example, olfactory neurons and mature T- and B-cells, can be reprogrammed into undifferentiated pluripotent cells by either somatic cell nuclear transfer or using the recently developed methodology for the generation of induced pluripotent stem cells (Takahashi and Yamanaka, 2006; Gurdon and Melton, 2008). Nevertheless, under normal nonmanipulated conditions *in vivo*, differentiated cells are remarkably stable, indicating the importance of mechanisms that maintain cells in their appropriate differentiated state. Gene targeting in non-neural cell types has revealed how transcription factors functioning in development can be important for the maintenance of terminally differentiated cell types, e.g., Pax5 in B-lymphocytes and Prox1 in lymphatic endothelial cells (Cobaleda et al., 2007; Johnson et al., 2008). In CNS, transcription factors identified for their key roles in early neuron development often continue to be expressed in the adult brain and may therefore guard against loss of phenotype or drift into alternative states (Smidt et al., 1997, 2000; Zetterström et al., 1997; Hendricks et al., 1999; Vult von Steyern et al., 1999; Albéri et al., 2004; Simon et al., 2004; Kang et al., 2007; Kittappa et al., 2007; Smidt and Burbach, 2007; Alavian et al.,

2008). However, remarkably little is known of how these factors function at late stages of development or in the adult. Although examples of adult mDA neuron loss has been reported in mice haploinsufficient for transcription factor genes such as *Engrailed* and *FoxA2*, it remains possible that defects originate during embryonic development (Albéri et al., 2004; Zhao et al., 2006; Kittappa et al., 2007; Sonnier et al., 2007). Importantly, FoxA2 and Engrailed are critical for the establishment of the floor plate and for early midbrain/hindbrain development, respectively, and they are directly and indirectly affecting many cell fates along the entire neuraxis. Thus, haploinsufficiency may cause embryonal deficiencies that do not become manifest until adult stages, a possibility that emphasizes the importance of temporally controlled conditional gene targeting to rigorously test how transcription factors function in terminally differentiated neurons.

We do not yet understand why Nurr1 is required in already differentiated mDA neurons. However, data presented here provide compelling evidence for the existence of "terminal selector genes" in mammalian CNS development. Such genes, defined from studies of *Caenorhabditis elegans* neuronal development, are continuously expressed throughout the life of neurons and are essential for both the establishment and maintenance of distinct neuronal phenotypes (Hobert, 2008). Thus, Nurr1, which probably regulates typical mDA neuron markers such as *TH*, *DAT*, *AADC*, and *VMAT2* (Sakurada et al., 1999; Sacchetti et al., 2001; Hermanson et al., 2003; Kim et al., 2003), is likely required for both early differentiation and maintenance by regulating genes that distinguish mDA neurons from other neuron types. Presumably, such regulation is critical throughout the life of mDA neurons and would depend on additional components, such as Pitx3, in a core transcription factor network (Jacobs et al., 2009).

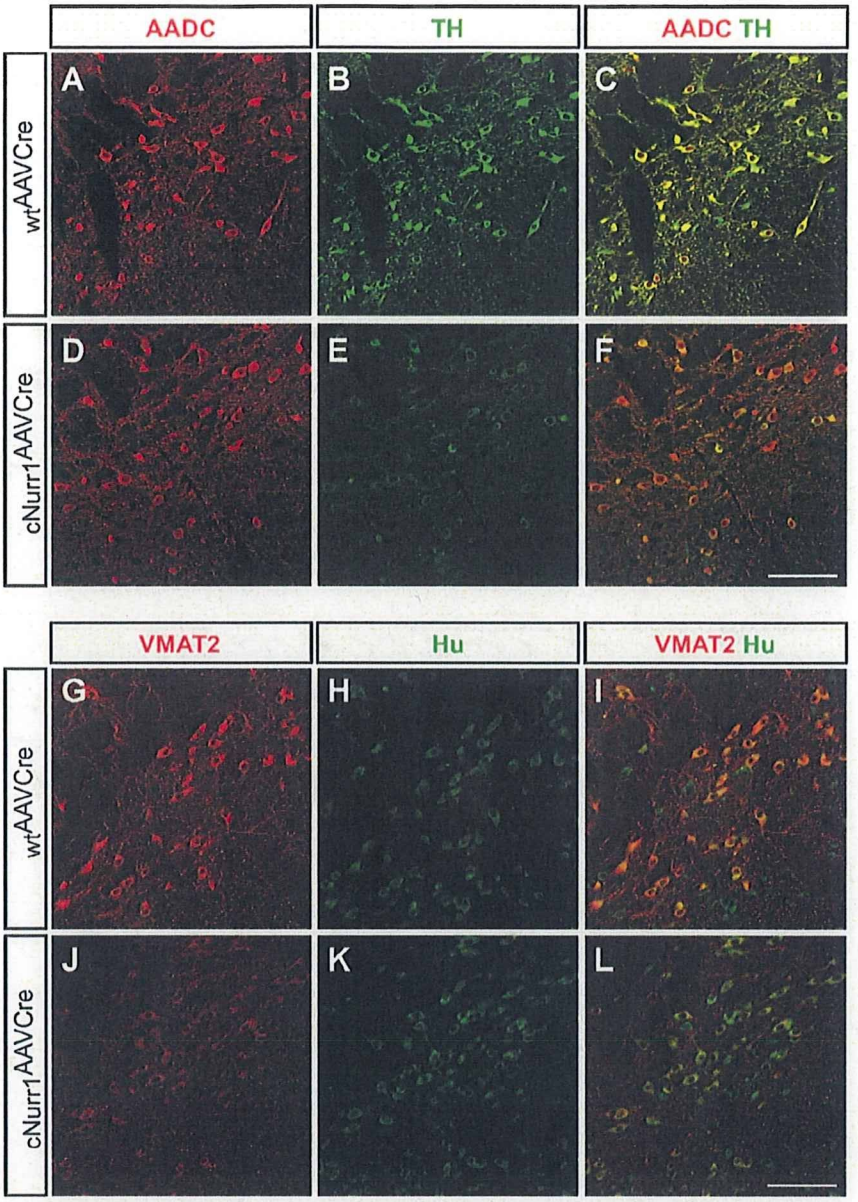

Figure 7. Decreased levels of VMAT2 but not AADC in $cNurr1^{AAVCre}$ mice. Confocal analysis of SNc in wt^{AAVCre} and $cNurr1^{AAVCre}$ mice at 4 months, as indicated. ***A–F***, Confocal images show staining of AADC (red; ***A***, ***D***), TH (green; ***B***, ***E***), and double staining of both markers (***C***, ***F***). Micrographs show that AADC expression appears expressed at normal levels in most cells with decreased levels of TH. ***G–L***, Confocal images show staining for VMAT2 (red; ***G***, ***J***), Hu (***H***, ***K***), and double staining of both markers (***I***, ***L***). Micrographs show that VMAT2 is severely decreased in $cNurr1^{AAVCre}$ mice, whereas Hu is maintained at normal levels in essentially all cells with decreased VMAT2. Scale bar, 200 μm.

How may dysregulated Nurr1 activity contribute to PD? Studies in PD patients have shown that, in early stages of the disease, SNc cell bodies are relatively spared compared with the loss of DA in the putamen (Fearnley and Lees, 1991) and that a significant fraction of the surviving, pigmented, DA somata in the SNc have much reduced expression of the TH enzyme (Hirsch et al., 1988; Chu et al., 2006). This suggests that, during early stages of disease, nigral DA neurons may survive in a dysfunctional state characterized by a downregulated neurotransmitter machinery. An interesting possibility supported by our data is that reduced expression of Nurr1 contributes to such symptoms. Indeed, Nurr1 is severely reduced in neurons with signs of pathology in PD brain tissue, and reduced Nurr1 expression in patients' peripheral blood lymphocytes indicates that diminished Nurr1 activity may be a systemic feature of disease (Chu et al., 2006; Le et al., 2008). Although such correlations do not determine whether reduced Nurr1 expression is a cause or a consequence of disease, progressive cell dysfunction in *Nurr1*-ablated mice provides a clear indication that diminished Nurr1 expression in PD should have deleterious consequences for patients. This view is supported by the identification of *Nurr1* gene variants that have been associated with rare cases of familial and sporadic PD (Xu et al., 2002; Le et al., 2003; Zheng et al., 2003; Jankovic et al., 2005; Grimes et al., 2006; Jacobsen et al., 2008). Although other studies have failed to identify such mutations and indicated that Nurr1

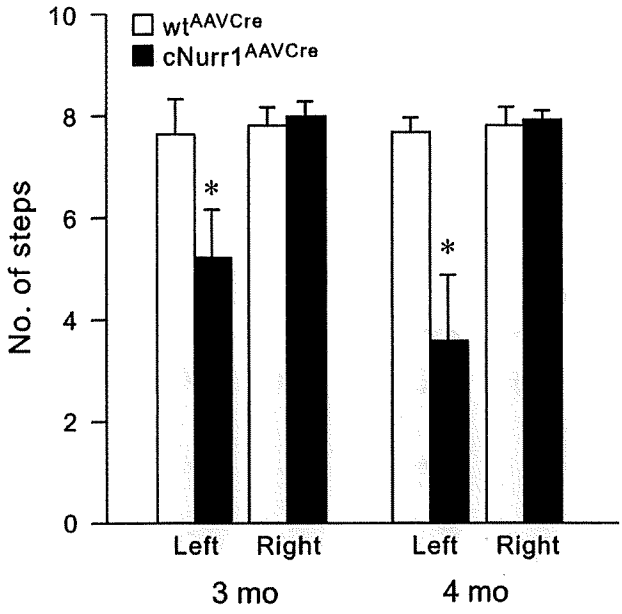

Figure 8. Forelimb akinesia in the stepping test. The performance of the left paw (contralateral to the vector injection) was significantly impaired in the fl/fl mice ($n = 16$) but not the wild-type mice ($n = 13$). Although the impairment was significant at both time points, 3 and 4 months after vector injection, their performance got significantly worse over time ($p < 0.01$, Student's paired t test): 15 of the 16 mice in the fl/fl group showed a decline in their stepping scores between the two tests, and at 4 months, 14 of the fl/fl mice had scores below 5 compared with 6 in the 3 month test. Scores give the means of steps recorded in the forehand and backhand direction for each paw (see Materials and Methods). *$p < 0.001$, Student's paired t test.

gene variants as a cause of PD must be very rare, the combined data from genetics, postmortem PD brain tissue analyses, and the ablation experiments reported here strongly imply that, if and when Nurr1 function is reduced, it will exaggerate PD progression and severity (Wellenbrock et al., 2003; Hering et al., 2004; Tan et al., 2004).

The results indicate that therapies that can restore Nurr1 activity in diseased but not yet degenerated mDA neurons could be of clinical relevance. We envision several strategies whereby Nurr1 activity could be increased. (1) Nurr1 belongs to the nuclear receptor family whose members are commonly regulated by small lipophilic ligands. The putative ligand binding domain of Nurr1 is unconventional and lacks a ligand-binding pocket, but Nurr1 forms heterodimers with retinoid X receptors (RXRs), and ligands activating these receptors can protect mDA neurons in culture (Wallen-Mackenzie et al., 2003; Wang et al., 2003). Thus, RXR may be a relevant target for ligand modulation of Nurr1-regulated processes. It will be important to investigate to what extent Nurr1–RXR heterodimers versus Nurr1 alone are important in pathways associated with the phenotype described in this paper. (2) Nurr1 activity is possible to modulate, for example, by the leukemia drug 6-mercaptopurine (Ordentlich et al., 2003). Although such drugs are pleiotropic and serious side effects are likely, other compounds with higher specificity may be possible to identify. (3) Therapies directed at increasing Nurr1 activity would be effective only as long as sufficient levels of Nurr1 are expressed in diseased neurons. Thus, treatments aimed at restoration of Nurr1 expression by gene delivery may prove advantageous. Using similar AAV vectors as administered in this study may be of particular interest because they have properties that are clinically favorable and are already used in clinical trials in PD patients (Check, 2007).

In conclusion, loss of Nurr1 at stages when characteristic features of mDA neurons are already apparent in the developing embryo or in fully differentiated adult neurons results in loss of mDA neuron-specific gene expression and neuron degeneration. These findings highlight the importance of developmental mechanisms also in the adult brain and clearly indicate that they may be critical for the understanding of cell maintenance and neurodegeneration. How Nurr1 and other transcription factors operate in adult neurons to control and prevent loss or drift in phenotype remains a challenge for future studies.

References

Alavian KN, Scholz C, Simon HH (2008) Transcriptional regulation of mesencephalic dopaminergic neurons: the full circle of life and death. Mov Disord 23:319–328.

Alberi L, Sgadò P, Simon HH (2004) Engrailed genes are cell-autonomously required to prevent apoptosis in mesencephalic dopaminergic neurons. Development 131:3229–3236.

Andersson E, Tryggvason U, Deng Q, Friling S, Alekseenko Z, Robert B, Perlmann T, Ericson J (2006) Identification of intrinsic determinants of midbrain dopamine neurons. Cell 124:393–405.

Breese GR, Knapp DJ, Criswell HE, Moy SS, Papadeas ST, Blake BL (2005) The neonate-6-hydroxydopamine-lesioned rat: a model for clinical neuroscience and neurobiological principles. Brain Res Brain Res Rev 48:57–73.

Castillo SO, Baffi JS, Palkovits M, Goldstein DS, Kopin IJ, Witta J, Magnuson MA, Nikodem VM (1998) Dopamine biosynthesis is selectively abolished in substantia nigra ventral tegmental area but not in hypothalamic neurons in mice with targeted disruption of the Nurr1 gene. Mol Cell Neurosci 11:36–46.

Check E (2007) Second chance. Nat Med 13:770–771.

Chu Y, Le W, Kompoliti K, Jankovic J, Mufson EJ, Kordower JH (2006) Nurr1 in Parkinson's disease and related disorders. J Comp Neurol 494:495–514.

Cobaleda C, Jochum W, Busslinger M (2007) Conversion of mature B cells into T cells by dedifferentiation to uncommitted progenitors. Nature 449:473–477.

Ekstrand MI, Terzioglu M, Galter D, Zhu S, Hofstetter C, Lindqvist E, Thams S, Bergstrand A, Hansson FS, Trifunovic A, Hoffer B, Cullheim S, Mohammed AH, Olson L, Larsson NG (2007) Progressive parkinsonism in mice with respiratory-chain-deficient dopamine neurons. Proc Natl Acad Sci U S A 104:1325–1330.

Fearnley JM, Lees AJ (1991) Ageing and Parkinson's disease: substantia nigra regional selectivity. Brain 114:2283–2301.

Grimes DA, Han F, Panisset M, Racacho L, Xiao F, Zou R, Westaff K, Bulman DE (2006) Translated mutation in the Nurr1 gene as a cause for Parkinson's disease. Mov Disord 21:906–909.

Gurdon JB, Melton DA (2008) Nuclear reprogramming in cells. Science 322:1811–1815.

Hendricks T, Francis N, Fyodorov D, Deneris ES (1999) The ETS domain factor Pet-1 is an early and precise marker of central serotonin neurons and interacts with a conserved element in serotonergic genes. J Neurosci 19:10348–10356.

Hering R, Petrovic S, Mietz EM, Holzmann C, Berg D, Bauer P, Woitalla D, Müller T, Berger K, Krüger R, Riess O (2004) Extended mutation analysis and association studies of Nurr1 (NR4A2) in Parkinson disease. Neurology 62:1231–1232.

Hermanson E, Joseph B, Castro D, Lindqvist E, Aarnisalo P, Wallén A, Benoit G, Hengerer B, Olson L, Perlmann T (2003) Nurr1 regulates dopamine synthesis and storage in MN9D dopamine cells. Exp Cell Res 288:324–334.

Hirsch E, Graybiel AM, Agid YA (1988) Melanized dopaminergic neurons are differentially susceptible to degeneration in Parkinson's disease. Nature 334:345–348.

Hobert O (2008) Regulatory logic of neuronal diversity: terminal selector genes and selector motifs. Proc Natl Acad Sci U S A 105:20067–20071.

Huot P, Parent A (2007) Dopaminergic neurons intrinsic to the striatum. J Neurochem 101:1441–1447.

Jacobs FM, van Erp S, van der Linden AJ, von Oerthel L, Burbach JP, Smidt MP (2009) Pitx3 potentiates Nurr1 in dopamine neuron terminal dif-

ferentiation through release of SMRT-mediated repression. Development 136:531–540.

Jacobsen KX, MacDonald H, Lemonde S, Daigle M, Grimes DA, Bulman DE, Albert PR (2008) A Nurr1 point mutant, implicated in Parkinson's disease, uncouples ERK1/2 dependent regulation of tyrosine hydroxylase transcription. Neurobiol Dis 29:117–122.

Jain S, Golden JP, Wozniak D, Pehek E, Johnson EM Jr, Milbrandt J (2006) RET is dispensable for maintenance of midbrain dopaminergic neurons in adult mice. J Neurosci 26:11230–11238.

Jankovic J, Chen S, Le WD (2005) The role of Nurr1 in the development of dopaminergic neurons and Parkinson's disease. Prog Neurobiol 77:128–138.

Johnson NC, Dillard ME, Baluk P, McDonald DM, Harvey NL, Frase SL, Oliver G (2008) Lymphatic endothelial cell identity is reversible and its maintenance requires Prox1 activity. Genes Dev 22:3282–3291.

Kang BJ, Chang DA, Mackay DD, West GH, Moreira TS, Takakura AC, Gwilt JM, Guyenet PG, Stornetta RL (2007) Central nervous system distribution of the transcription factor Phox2b in the adult rat. J Comp Neurol 503:627–641.

Kim KS, Kim CH, Hwang DY, Seo H, Chung S, Hong SJ, Lim JK, Anderson T, Isacson O (2003) Orphan nuclear receptor Nurr1 directly transactivates the promoter activity of the tyrosine hydroxylase gene in a cell-specific manner. J Neurochem 85:622–634.

Kirik D, Rosenblad C, Björklund A (1998) Characterization of behavioral and neurodegenerative changes following partial lesions of the nigrostriatal dopamine system induced by intrastriatal 6-hydroxydopamine in the rat. Exp Neurol 152:259–277.

Kittappa R, Chang WW, Awatramani RB, McKay RD (2007) The foxa2 gene controls the birth and spontaneous degeneration of dopamine neurons in old age. PLoS Biol 5:e325.

Kramer ER, Aron L, Ramakers GM, Seitz S, Zhuang X, Beyer K, Smidt MP, Klein R (2007) Absence of Ret signaling in mice causes progressive and late degeneration of the nigrostriatal system. PLoS Biol 5:e39.

Le W, Pan T, Huang M, Xu P, Xie W, Zhu W, Zhang X, Deng H, Jankovic J (2008) Decreased NURR1 gene expression in patients with Parkinson's disease. J Neurol Sci 273:29–33.

Le WD, Xu P, Jankovic J, Jiang H, Appel SH, Smith RG, Vassilatis DK (2003) Mutations in NR4A2 associated with familial Parkinson disease. Nat Genet 33:85–89.

Oo TF, Kholodilov N, Burke RE (2003) Regulation of natural cell death in dopaminergic neurons of the substantia nigra by striatal glial cell line-derived neurotrophic factor *in vivo*. J Neurosci 23:5141–5148.

Ordentlich P, Yan Y, Zhou S, Heyman RA (2003) Identification of the antineoplastic agent 6-mercaptopurine as an activator of the orphan nuclear hormone receptor Nurr1. J Biol Chem 278:24791–24799.

Pascual A, Hidalgo-Figueroa M, Piruat JI, Pintado CO, Gómez-Díaz R, López-Barneo J (2008) Absolute requirement of GDNF for adult catecholaminergic neuron survival. Nat Neurosci 11:755–761.

Perlmann T, Wallén-Mackenzie A (2004) Nurr1, an orphan nuclear receptor with essential functions in developing dopamine cells. Cell Tissue Res 318:45–52.

Sacchetti P, Brownschidle LA, Granneman JG, Bannon MJ (1999) Characterization of the 5′-flanking region of the human dopamine transporter gene. Brain Res Mol Brain Res 74:167–174.

Sacchetti P, Mitchell TR, Granneman JG, Bannon MJ (2001) Nurr1 enhances transcription of the human dopamine transporter gene through a novel mechanism. J Neurochem 76:1565–1572.

Sakurada K, Ohshima-Sakurada M, Palmer TD, Gage FH (1999) Nurr1, an orphan nuclear receptor, is a transcriptional activator of endogenous tyrosine hydroxylase in neural progenitor cells derived from the adult brain. Development 126:4017–4026.

Saucedo-Cardenas O, Quintana-Hau JD, Le WD, Smidt MP, Cox JJ, De Mayo F, Burbach JP, Conneely OM (1998) Nurr1 is essential for the induction of the dopaminergic phenotype and the survival of ventral mesencephalic late dopaminergic precursor neurons. Proc Natl Acad Sci U S A 95:4013–4018.

Schallert T, Norton D, Jones TA (1992) A clinically relevant unilateral rat model of Parkinsonian akinesia. J Neural Transpl Plast 3:332–333.

Simon HH, Thuret S, Alberi L (2004) Midbrain dopaminergic neurons: control of their cell fate by the engrailed transcription factors. Cell Tissue Res 318:53–61.

Smidt MP, Burbach JP (2007) How to make a mesodiencephalic dopaminergic neuron. Nat Rev Neurosci 8:21–32.

Smidt MP, van Schaick HS, Lanctôt C, Tremblay JJ, Cox JJ, van der Kleij AA, Wolterink G, Drouin J, Burbach JP (1997) A homeodomain gene Ptx3 has highly restricted brain expression in mesencephalic dopaminergic neurons. Proc Natl Acad Sci U S A 94:13305–13310.

Smidt MP, Asbreuk CH, Cox JJ, Chen H, Johnson RL, Burbach JP (2000) A second independent pathway for development of mesencephalic dopaminergic neurons requires Lmx1b. Nat Neurosci 3:337–341.

Smidt MP, Smits SM, Burbach JP (2004) Homeobox gene Pitx3 and its role in the development of dopamine neurons of the substantia nigra. Cell Tissue Res 318:35–43.

Snyder AM, Zigmond MJ, Lund RD (1986) Sprouting of serotoninergic afferents into striatum after dopamine-depleting lesions in infant rats: a retrograde transport and immunocytochemical study. J Comp Neurol 245:274–281.

Sonnier L, Le Pen G, Hartmann A, Bizot JC, Trovero F, Krebs MO, Prochiantz A (2007) Progressive loss of dopaminergic neurons in the ventral midbrain of adult mice heterozygote for Engrailed 1. J Neurosci 27:1063–1071.

Soriano P (1999) Generalized lacZ expression with the ROSA26 Cre reporter strain. Nat Genet 21:70–71.

Takahashi K, Yamanaka S (2006) Induction of pluripotent stem cells from mouse embryonic and adult fibroblast cultures by defined factors. Cell 126:663–676.

Tan EK, Chung H, Chandran VR, Tan C, Shen H, Yew K, Pavanni R, Puvan KA, Wong MC, Teoh ML, Yih Y, Zhao Y (2004) Nurr1 mutational screen in Parkinson's disease. Mov Disord 19:1503–1505.

Vult von Steyern F, Martinov V, Rabben I, Njå A, de Lapeyrière O, Lømo T (1999) The homeodomain transcription factors Islet 1 and HB9 are expressed in adult alpha and gamma motoneurons identified by selective retrograde tracing. Eur J Neurosci 11:2093–2102.

Wallen-Mackenzie A, Mata de Urquiza A, Petersson S, Rodriguez FJ, Friling S, Wagner J, Ordentlich P, Lengqvist J, Heyman RA, Arenas E, Perlmann T (2003) Nurr1-RXR heterodimers mediate RXR ligand-induced signaling in neuronal cells. Genes Dev 17:3036–3047.

Wang Z, Benoit G, Liu J, Prasad S, Aarnisalo P, Liu X, Xu H, Walker NP, Perlmann T (2003) Structure and function of Nurr1 identifies a class of ligand-independent nuclear receptors. Nature 423:555–560.

Wellenbrock C, Hedrich K, Schafer N, Kasten M, Jacobs H, Schwinger E, Hagenah J, Pramstaller PP, Vieregge P, Klein C (2003) NR4A2 mutations are rare among European patients with familial Parkinson's disease. Ann Neurol 54:415.

Xu PY, Liang R, Jankovic J, Hunter C, Zeng YX, Ashizawa T, Lai D, Le WD (2002) Association of homozygous 7048G7049 variant in the intron six of Nurr1 gene with Parkinson's disease. Neurology 58:881–884.

Zetterström RH, Williams R, Perlmann T, Olson L (1996) Cellular expression of the immediate early transcription factors Nurr1 and NGFI-B suggests a gene regulatory role in several brain regions including the nigrostriatal dopamine system. Brain Res Mol Brain Res 41:111–120.

Zetterström RH, Solomin L, Jansson L, Hoffer BJ, Olson L, Perlmann T (1997) Dopamine neuron agenesis in Nurr1-deficient mice. Science 276:248–250.

Zhao ZQ, Scott M, Chiechio S, Wang JS, Renner KJ, Gereau RW 4th, Johnson RL, Deneris ES, Chen ZF (2006) Lmx1b is required for maintenance of central serotonergic neurons and mice lacking central serotonergic system exhibit normal locomotor activity. J Neurosci 26:12781–12788.

Zheng K, Heydari B, Simon DK (2003) A common NURR1 polymorphism associated with Parkinson disease and diffuse Lewy body disease. Arch Neurol 60:722–725.

ALSにおけるRNA editing異常

日出山 拓人（ひでやま たくと） 東京大学大学院医学系研究科脳神経医学専攻神経内科学
東京大学保健・健康推進本部
郭 伸（かく しん） 東京大学大学院准教授
医学系研究科脳神経医学専攻神経内科学

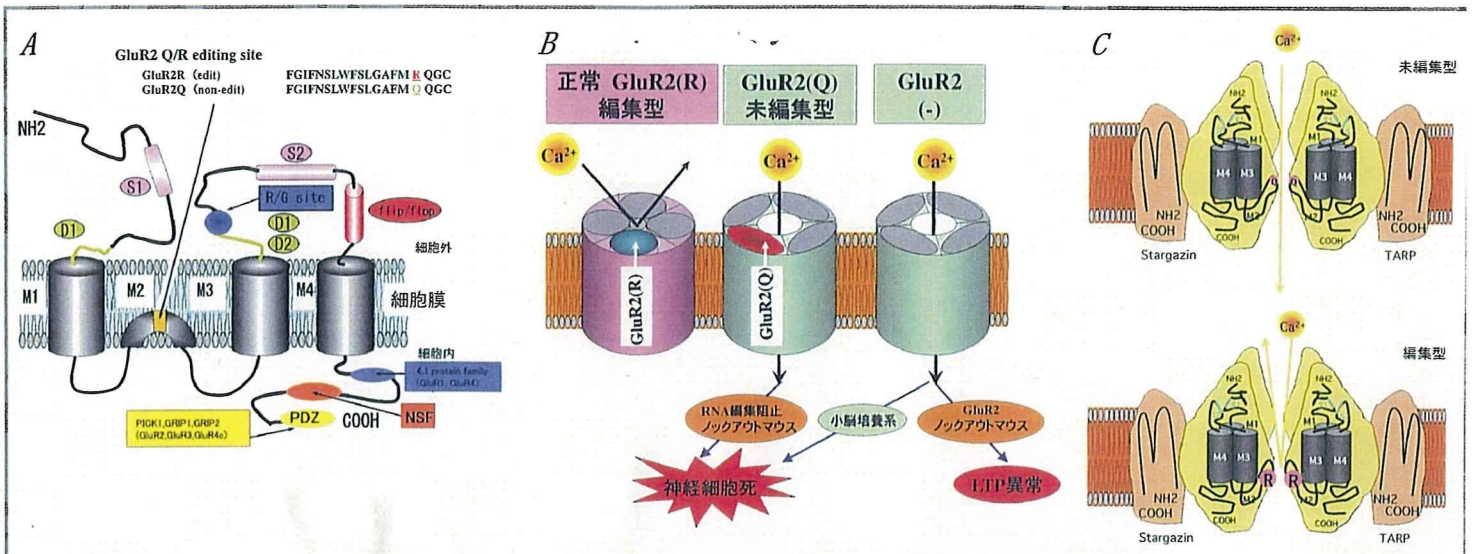

図1 GluR2サブユニットとCa^{2+}透過性による興奮性神経細胞死

A）AMPA受容体の各サブユニットのM2にはQ/R部位と呼ばれる部位があり，同部位はGluR2以外ではグルタミン(Q)であるのに対して，GluR2だけはアルギニン(R)である．しかしゲノムレベルでは，GluR2もQをコードしているCAGという配列である．Rとなる理由はRNAへ転写後，mRNAになる前にアデノシン(A)がイノシン(I)へと塩基置換され，CAG(Q)からCIG(R)へのアミノ酸置換が生じるためである．リボソームでIはグアノシン(G)と同等であると見なされるため，CIGはCGGと見なされRとして翻訳される．この現象はRNA編集と呼ばれる．B）サブユニットの中で，チャネルのCa^{2+}透過性決定に重要な役割を果たしているのはGluR2である．AMPA受容体のCa^{2+}透過性はGluR2の有無によって決定されている．AMPA受容体を構成する4つのサブユニットのうちGluR2を1つ以上含む受容体は，Ca^{2+}透過性が低いのに対し，Glu R1，3，4のサブユニットだけで構成された受容体は，高いCa^{2+}透過性を示す．C）Q/R部位がCa^{2+}透過性決定に重要なのはチャネルポアに面しており，陽電化のRがCa^{2+}を弾くのに対して電気的に中性のQではこの作用が弱いためであると考えられている．

はじめに

筋萎縮性側索硬化症(amyotrophic lateral sclerosis：ALS)は，90%が家族歴を認めない孤発性で，原因不明かつ治療方法のない神経変性疾患である．著者らは，孤発性ALS脊髄運動ニューロンでは，グルタミン酸受容体であるAMPA(α-3-hydroxy-5-methyl-4-isoxazole propionic acid)受容体チャネルのCa^{2+}透過性を亢進させる分子変化が疾患特異的，細胞選択的に起こっていることを見出し，この分子変化が神経細胞死の直接原因になることから，ALSの病因と考えられることを明らかにした[1]．この分子変化を生じる上流の現象がRNA編集(RNA editing)である．

孤発性ALSにおける興奮性神経細胞死とAMPA受容体

錐体路の神経伝達物質はグルタミン酸で，脊髄運動ニューロンもグルタミン酸受容体が豊富に発現する．グルタミン酸による興奮が過剰になるとイオン透過性亢進により内部恒常性の破綻を来し，細胞死のカスケードが働く，というのが興奮性神経細胞死のメカニズムである．主に興奮性神経細胞死は，虚血や低血糖，外傷，てんかん重積などの急性の神経細胞死に働くと考えられていた．一方で，培養細胞系，*in vivo*動物実験系で急性には神経細胞死を引き起こさない薄い濃度でも，受容体が長期間持続的に興奮することで遅発性の神経細胞死が起こることが明らかにされた．このことから，慢性に進行する神経変性疾患であるALSにおいて遅発性の神経細胞死の関与が注目されるようになった．さらに，運動ニューロンは興奮性細胞死に脆弱であり，過剰なCa^{2+}流入による細胞内Ca^{2+}濃度の持続的上昇が細胞死の原因と考えられている．神経細胞内Ca^{2+}濃度上昇の機構にはAMPA受容体のCa^{2+}透過性の関与が大きい．

AMPA受容体とRNA編集

AMPA受容体は4種のサブユニット(GluR1-4)の単独，または様々な組み合わせからなる四量体である．AMPA受容体のCa^{2+}透過性を決定する因子には，GluR2サブユニット，GluR2サブユニットのRNA編集(特にQ/R部位)，flip/flop splicing varient，AMPA受容体密度が挙げられる．しかし，Ca^{2+}透過性を規定する因子の全てが細胞死に直接関連するわけではない．GluR2のノックアウトにより小脳培養系では細胞死が生じるが[2]，GluR2ノックアウトマウスではLTP異常のみで細胞死は生じない[3]（図1B）．Flip/flop isoformは細胞死を生じないが，AMPA受容体毒性を強める[4]．AMPA受容体密度の変化のみでは神経細胞死を生じない[5]．これに対し，RNA編集を阻止した変異マウスでは生後20日以内に痙攣による個体死が認められる[6]（図1B）．

AMPA受容体サブユニット発現とALSの運動ニューロン死

これらの結果をふまえ，神経細胞死に関連する分子変化であるGluR2の減少ないしGluR2 Q/R部位の編集率低下の有無を著者らのグループは検討した．Kwakらはlaser microdissectorを用いて凍結剖検脊髄組織から単一運動神経細胞を切り出し，RT-PCR法によりGluR2 mRNA由来のcDNAを増幅し，AMPA受容体各サブユニットmRNAを定量する方法およびGluR2 Q/R部位RNA編集率を定量する方法を確立した．そして，孤発性ALS脊髄運動

0289-0585/10/¥500/論文/JCOPY

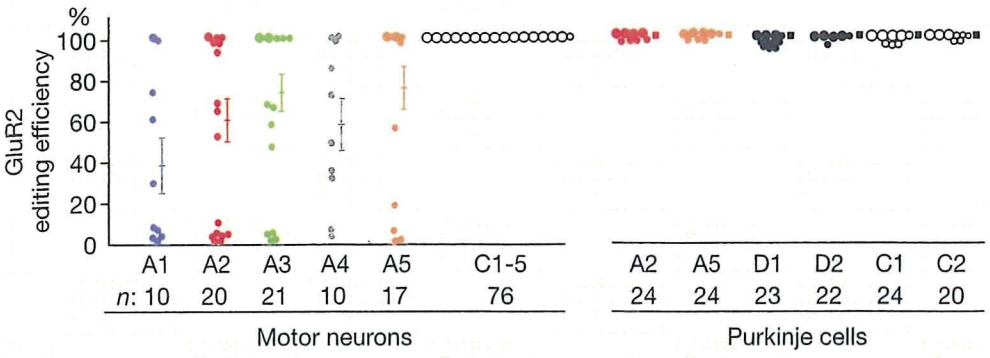

図 2　単一神経細胞における GluR2 Q/R 部位 RNA 編集率
(Kawahara ら[1]より改変)

各点(大きな点は 5 細胞，小さな点は 1 細胞)は，ALS 群 5 例(A1-A 5)，コントロール群 5 例(C 1-C 5)の単一脊髄運動ニューロンにおける GluR2 Q/R 部位の RNA 編集率と，ALS 群 2 例(A 2, A 5)，Dentatorubral-pallidoluysian atrophy(DRPLA)群 2 例(D 1, D 2)，コントロール群 2 例(C 1，C 2)の単一小脳プルキンエ細胞の編集率を表している．平均値±標準誤差と解析した細胞数(n)も示した．運動ニューロンにおける正常コントロール 76 個の内訳は，C 1：28，C 2：12，C 3：13，C 4：12，C 5：11 である．運動ニューロンでは正常コントロール群のすべての細胞において，例外なく編集率は 100%であった．これに対して，ALS 群では解析した 5 例すべてにおいて，編集率は 0～100%まで大きくばらつき，正常コントロール群と比較し有意に低下していた(Mann-Whitney U test，$p<0.001$)．一方，小脳プルキンエ細胞における編集率については，ALS 群，DRPLA 群とコントロール群の間には有意差はない(Mann-Whitney U test，$p>0.05$)．また，他の変性疾患の病変組織や他の運動ニューロン病(SBMA)では，編集率の低下は認めない．このような選択特異性を生む機序としては，脊髄運動ニューロンの AMPA 受容体総 mRNA 発現量および GluR2 サブユニット比率が，他のニューロンに比べて低く，もともと Ca^{2+} 透過性 AMPA 受容体の割合が多いこと，したがって RNA 編集低下の影響を受けやすいことが挙げられる．

表；既知の A→I RNA 編集部位および神経・精神疾患

	基質名	編集部位	編集により変化する性質	マウス全脳由来 mRNA 編集効率	担当酵素	疾患との関連
AMPA 型グルタミン酸受容体	GluR2	Q/R 部位	受容体チャネルの Ca^{2+} 透過性	100%	ADAR2	ALS(編集効率低下) 悪性膠芽腫(編集効率低下*)
	GluR2, GluR3, GluR4	R/G 部位	受容体チャネルの脱感作時間	GluR2：75%，GluR3：90%，GluR4：45%	ADAR1，ADAR2	
カイニン酸型グルタミン酸受容体	GluR5	Q/R 部位	受容体チャネルの Ca^{2+} 透過性	64%	ADAR1，ADAR2	
	GluR6	Q/R 部位，I/V 部位，Y/C 部位	受容体チャネルの Ca^{2+} 透過性	Q/R 部位：86%，I/V 部位：87%，Y/C 部位：90%	ADAR1，ADAR2	側頭葉てんかん (Glu R6 Q/R 部位編集効率上昇)
セロトニン受容体	5-HT_{2C}R	A～E 部位	G タンパク結合効率	A 部位：75%，B 部位：80%，C 部位：15%，D 部位：70%，E(C′)部位	A，B 部位：ADAR1，C，D 部位：ADAR2	うつ病 (5-HT_{2C}受容体 D，E 部位編集効率上昇)
膜電位依存型カリウムチャネル	Kv 1.1	S 6 ドメイン内	チャネルの不活化	48%	ADAR2	Episodic ataxia type I (編集異常は不明)**
RNA 編集酵素	ADAR2	自己編集部位	酵素活性	15%	ADAR2	

*正常の白質組織と比較すると低下していない．**本態は point mutation であり，RNA 編集異常の関与が考えられている．

RNA 編集の意義としては，RNA 編集により特定のアミノ酸が置換され，翻訳産物の大きさや分子配列が変化することで翻訳産物が別の機能を獲得する場合がある．RNA 編集は，シトシン(C)→ウラシル(U)とアデノシン(A)→イノシン(I)の 2 種類が知られている．C→U の RNA 編集は植物から哺乳類まで保存され，植物ミトコンドリアのある遺伝子には開始コドンがないが，ACG→AUG と編集されることにより開始コドンが出来，翻訳可能な配列になる correctional editing などが知られている．哺乳類では C→U 編集は活発ではない．A→I 編集は中枢神経系で活発に起こっており，ヒト D 型肝炎ウイルス，線虫，ショウジョウバエ，イカ，哺乳類で確認されており，太古から存在している現象と考えられる．GluR2 Q/R 部位が哺乳類で最初に見つかった編集部位であり，この他に，表のように編集部位は受容体やイオンチャネルに多く見られ，R/G 部位は胎児発生の過程で徐々に増加し，イオンチャネルの脱感作を調節し，GluR6 の I/V，Y/C 部位はイオンチャネルの電気抵抗性に関与している．神経変性疾患の他，てんかん，精神疾患(統合失調症，うつ病，自殺)，遺伝性皮膚疾患(遺伝性対側性色素異常症)での検討が行われているが，現時点でヒトの疾患との関連が明らかにされたものは，著者らのグループで発見した ALS の運動ニューロンのみである．

ニューロンの単一神経細胞レベルで，GluR2 mRNA 発現量に有意な減少がないこと[7]，および ALS の単一運動ニューロンに GluR2 Q/R 部位 RNA 編集率低下という RNA 編集異常が細胞選択的かつ疾患特異的に見られることを報告した[1,8](図 2)．

RNA 編集と RNA 編集酵素 ADAR2

この GluR2 Q/R 部位の RNA 編集を特異的に制御しているのが RNA 編集酵素 adenosine deaminase acting on RNA type 2(以下 ADAR2)である[9]．一般に，あるタンパクへと翻訳される mRNA は遺伝子から転写された後，スプライシングを受け，イントロン部分が切り出されて形成される．遺伝情報は正確に転写されなければ生死に関わるような重大な障害を来す可能性があるが，遺伝子から mRNA が形成される過程で遺伝情報が書き換えられることがある．これを RNA 編集(RNA editing)と呼ぶ[10]．RNA 編集のうち特に転写後のコドン置換を伴う場合には，タンパクの機能を変える場合があり，生物学的にも重要な反応である．孤発性 ALS で認められるような A→I 編集は中枢神経系で最も活発に生じている(表参照)．中でも GluR2 の Q/R 部位は，胎生期から成熟期に至るまでほぼ 100%編集されているという点で特異的であり，これほど高い編集率を示す部位は他には見いだされていない．

著者らのグループは ADAR2 コンディショナルノックアウトマウスを作成し，神経細胞死を生じるかどうか検討中であり，ADAR2 の機能解明が孤発性 ALS の治療方法開発につながると期待している．

文　献

1) Kawahara Y, et al. Nature. 2004；427：801.
2) Iihara K, et al. J Neurosci. 2001；21：2224-39.
3) Jia Z, et al. Neuron. 1996；17：945-56.
4) Sun H, et al. J Neurochem. 2006；98：782-91.
5) Kwak S, et al. J Mol Med. 2005；83：110-20.
6) Brusa R, et al. Science. 1995；270：1677-80.
7) Kawahara Y, et al. J Neurochem. 2003；85：680-9.
8) Takuma H, et al. Ann Neurol. 1999；46：806-15.
9) Higuchi M, et al. Nature. 2000；406：78-81.
10) Keegan LP, et al. Nat Rev Genet. 2001；2：869-78.

1. グルタミン酸受容体と孤発性筋萎縮性側索硬化症

日出山拓人，山下雄也，郭　伸

孤発性筋萎縮性側索硬化症（amyotrophic lateral sclerosis，以下ALS）は，原因不明の神経変性疾患である．近年，私たちのグループではグルタミン酸受容体サブユニットであるGluR2のRNA編集異常が疾患特異的に生じていることを，孤発性ALS例と疾患対照，正常対照例の検討から明らかにした．これは原因解明とともに疾患特異的な治療方法を開発できる可能性を示唆するものである．本稿では，これまでの歴史的な経緯と最近の知見について述べてみたい．

はじめに：筋萎縮性側索硬化症とは

筋萎縮性側索硬化症（amyotrophic lateral sclerosis：以下，ALS）は，運動ニューロンがある時期から変性に陥る，原因不明で治療法のない神経変性疾患である．ALSの発症率は人口10万人あたり0.8～7.3人/年程度，有病率は2～8人程度であり頻度や人種差は認められていないため，共通の発生機序の存在が示唆される．臨床的に典型例では一側上肢の遠位部小手筋から筋力低下・筋萎縮が始まる．やがて嚥下障害，呼吸筋麻痺などによって，多くは2～5年（平均3年）程度で死に至る難病である．

病理学的には，脊髄前角にも側索にもグリオーシスを認め，脊髄前角の大型運動ニューロンの脱落が著明である．残存ニューロン内には，Bunina小体と呼ばれるエオジン好性のシスタチン抗体陽性，トランスフェリン抗体陽性の細胞内封入体やユビキチン陽性，TDP-43陽性封入体であるskein-like inclusionやLewy body-like hyaline inclusionなどの封入体がみられる．

孤発性ALSは全患者の90％以上を占め，既知の家族性ALSの責任遺伝子異常は大多数の症例で見出されていないため，家族性ALSとは発症メカニズムが異な

[キーワード＆略語]
RNA編集，AMPA受容体，ALS，GluR2，Q/R部位

ALS：amyotrophic lateral sclerosis（筋萎縮性側索硬化症）
AMPA：α-3-hydroxy-5-methyl-4-isoxazole propionic acid
DRPLA：dentatorubropallidoluysian atrophy（歯状核赤核淡蒼球ルイ体萎縮症）
MSA：multiple system atrophy(多系統萎縮症)
ADAR：adenosine deaminase acting on RNA
ECS：exon complementary sequence
CYFIP：cytoplasmic fragile X mental retardation protein interacting protein

AMPA receptor and sporadic amyotrophic lateral sclerosis
Takuto Hideyama[1)2)]/Takenari Yamashita[1)]/Shin Kwak[1)]：Department of Neurology, University of Tokyo, Graduate School of Medicine[1)]/Division for Health Service Promotion, University of Tokyo[2)]（東京大学大学院医学系研究科脳神経医学専攻神経内科学[1)]/東京大学保健・健康推進本部[2)]）

ると考えられる．中毒説，神経栄養因子欠乏説，細胞骨格タンパク異常説，逆行性軸索流異常説などが検討されてきたが，いずれも証明されていない．このような状況の中，Kwakらによって孤発性ALS脊髄運動ニューロンでは，グルタミン酸受容体であるAMPA（α-3-hydroxy-5-methyl-4-isoxazole propionic acid）受容体サブユニットの1つであり，Ca^{2+}透過性AMPA受容体を構成するGluR2のQ/R部位にRNA編集が起こらない未編集型のGluR2増加が，疾患特異的，細胞選択的に起こっていることが発見された[1]．

1 AMPA受容体と興奮性神経細胞死

1）グルタミン酸による遅発性興奮性細胞死

錐体路はグルタミン酸が神経伝達物質であり，脊髄運動ニューロンもこの興奮性入力を豊富に受けている．そのため運動ニューロンにおいてもグルタミン酸受容体が高密度で発現している．興奮性神経細胞死のメカニズムは，グルタミン酸による興奮が過剰になるとCa^{2+}などのイオン透過性亢進が引き起こされ，内部恒常性が破綻し，細胞死のカスケードが働くというものである．興奮性神経細胞死は，主に虚血や低血糖，外傷，てんかん重積などの急性の神経細胞死に働くと考えられていた．一方で，培養細胞系，*in vivo*動物実験系で急性には神経細胞死を引き起こさない低い濃度でもAMPA受容体が長期間持続的に興奮することで遅発性の神経細胞死が起こることが次々と明らかにされ，特にALSでAMPA受容体を介する神経細胞死がALSの神経細胞死に働いていることを支持する結果が得られている[2)3)]．次に，AMPA受容体の特性と神経細胞死について論じる．

2）神経細胞死とAMPA受容体

グルタミン酸受容体は大きくイオンチャネル型と代謝調節型に分類される．そしてイオンチャネル型はさらにNMDA受容体，カイニン酸受容体，AMPA受容体に分けられる．NMDA受容体が急性の神経細胞死に関与するのに対して，AMPA受容体は速いシナプス伝達に関わるニューロンの遅発性細胞死に関与し，運動ニューロンは，特に後者の興奮性細胞死に脆弱であることが知られている．その分子メカニズムとして細胞死のトリガーとなるのは，過剰なCa^{2+}流入による細胞内Ca^{2+}濃度の持続的上昇である．神経細胞内Ca^{2+}濃度上昇の機構には，①NMDA受容体の活性化によるチャネルからのCa^{2+}流入，②Ca^{2+}透過性AMPA受容体の活性化，③代謝型グルタミン酸受容体などの興奮によるIP3産生を介する小胞体からのCa^{2+}動員，④膜の脱分極による膜電位依存性Ca^{2+}チャネルの開口などのメカニズム，⑤電位非依存性カチオン透過性チャネルの関与（transient receptor potential）が知られている．特にラット培養脊髄神経細胞の検討などから②のAMPA受容体を介した経路が重要であることがわかった．オートラジオグラフや免疫組織学的検討から，ヒトや動物の脊髄運動ニューロンには，カイニン酸受容体の発現が乏しいのに対して，AMPA受容体は豊富に発現しており，膜電位決定は主にAMPA受容体が担っている．また，ALS患者髄液を培養ラット皮質神経細胞に投与すると神経細胞死が生じ，AMPA受容体アンタゴニストによってレスキューできるがNMDA受容体アンタゴニストによっては防げないなど，NMDA受容体よりAMPA受容体を介した細胞死に脆弱であることが示されている[4]．

3）AMPA型受容体のCa^{2+}透過性決定因子

AMPA受容体は，電気生理，化学量論，超微形態など，多方面からの検討により4種のサブユニット（GluR1-GluR4）の単独またはさまざまな組み合わせからなる四量体と考えられている．各サブユニットは共通構造を持っており，相互に約70％のアミノ酸配列の相同性を持つ（**図1 A**）．

AMPA受容体のCa^{2+}透過性を決定する因子には，①GluR2サブユニット，②GluR2サブユニットのRNA編集（特にQ/R部位），③flip/flop splicing variantやR/G部位の編集率などチャネルの開口を編集するドメインがあり，細胞全体としては④AMPA受容体密度もCa^{2+}流入量を決定する大きな因子となる．しかし，Ca^{2+}透過性を規定する因子のすべてが細胞死に直接関連するわけではない．GluR2のノックアウトにより小脳培養系では細胞死が生じるが[5]，GluR2ノックアウトマウスではLTP異常のみで細胞死は生じない[6]．flip/flop isoformは，細胞死を生じないが，AMPA受容体毒性を強める[7]．AMPA受容体密度の変化のみでは神経細胞死を生じない[8]．これに対し，RNA編集を阻止した変異マウスでは生後20日以内に痙攣により死亡する[9]（**図1 B**）．